QAM Digital Communications ©

By

Raymond L. Barrett, Jr., PhD, PE
CEO, American Research and Development, LLC

 Copyright© 2010 Raymond L. Barrett, Jr.

1.0 QAM Digital Communications Introduction and Basic Models

This course introduces “Suppressed Carrier” modulation and introduces the Weaver modulator architecture developed for “Single-Sideband, Suppressed Carrier” analog voice applications. The Weaver architecture has been in the public domain for more than 40 years and the subject of many variations leading to other applications, too. We add phase modulation and amplitude modulation to the Weaver architecture showing the development of quadrature techniques for using both upper and lower Weaver sidebands to produce independent “I” and “Q” communications channels. Only one bit of information is discussed for each of the phase modulation and amplitude modulation in a simple QAM example, but the groundwork is laid for extending the system. The concept of symbol rate and bit rates is introduced. The importance of frequency and phase synchronization of the receiving Weaver modulator is introduced and examples of issues discussed.

The availability of powerful digital signal processor techniques has driven communications systems into the digital realm. Most of the communications media are still continuous and fundamentally analog in nature and the digital information is modulated onto a carrier for transport in the medium. Analog techniques utilize sine wave signals in and Fourier or Laplace mathematics to describe signals and systems. Digital techniques utilize discrete-time and magnitudes that produce square wave or Zero-Order Hold “stairstep” waveform signals. The consequence of using digital signals in an analog medium is the presence of energy at harmonically related frequencies. We illustrate the need for selectively removing or retaining the harmonic energy at different stages of the communications process. The consequence of ignoring some harmonic generation by digital processes results in unintended errors and interference to other services. One remedy for suppression of unwanted harmonic energy is to employ frequency selective filtering at various stages prior to delivery of the output to the medium. The filtering can be implemented using analog or filter digital techniques at each location within the capabilities of either technique. Inherent in the process of frequency selectivity is the possible consequence of frequency dependent group delay and the amplitude modulation envelope distortions it can cause.

 Copyright© 2010 Raymond L. Barrett, Jr.

2.0 Signal/System Classification-

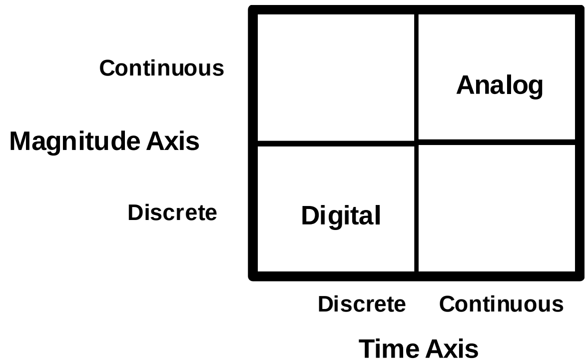

Figure 2.0 Signal/System Classification Matrix

Analog signals exist at all instances of time and can take on a continuous range of magnitude values over some range of interest. Digital signals, however, have a finite set of discrete values that are used to describe the magnitudes and can only change those values at discrete time instances. The digital signals are most often converted to a continuous representation for use in an analog medium in a "stair-step" fashion using a "Zero-Order Hold" (ZOH) function between the discrete-time instances.

In the 1940s, Claude Shannon developed the concept of "channel capacity" to relate the capacity of a channel to carry information. His famous result is repeated in equation [2.1] below as:

$$C = BW \log_2 (1 + SNR) \qquad [2.1]$$

The "capacity" (C) of a channel is equal to the bandwidth (BW) of that channel and the logarithm (to the base 2) of 1 plus the Signal-to-Noise Ratio (SNR). His work is the foundation for "Information Theory" and is an "existence" statement for the existence of a code to achieve the result stated. Shannon says the codes exist for retrieving bits coded for the channel without saying what the codes are. We accept his statement without proof or example, but use the result to show why communications is migrating from analog to digital forms. In any given bandwidth, an analog signal that acquires a "noise" from the channel or the devices used in the implementation cannot become any "better" as it is propagated. A digital signal, however, can be retrieved from a channel, restored to an error-free condition and either used or re-transmitted. The used of digital information in an analog transmission medium can overcome the SNR degradations of analog propagation. The digital signals can

 Copyright© 2010 Raymond L. Barrett, Jr.

be in a code that maintains Signal to Noise Ratio (SNR) at a favorable value, whereas the analog signals degrade without such effects.

3.0 Analog Media/Signal Representation using Sinusoids

Classical Analog systems decompose signals as sinusoids for periodic steady-state analysis. The choice of representation of signals is associated with the use of Fourier and Laplace Transform techniques for System descriptions. Digital signals, too, can be described but as a summation of sinusoids in a wide-bandwidth representation.

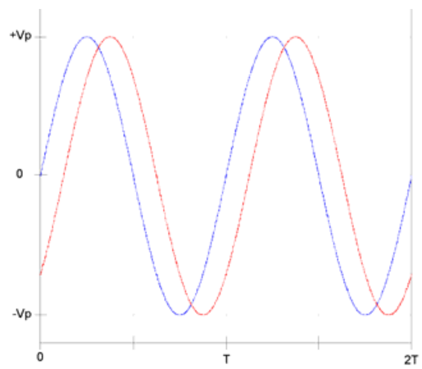

Figure 3.0 Two Sinusoids with the same Period and a Phase Difference

In Figure 3.0 above, each sinusoid is at the same frequency (***F***) expressed in Hertz and related to the Period (***T***) by $F = 1/T$.

In the illustration, each sinusoid is identical except for the difference in the time when each waveform rises through a value of zero magnitude. That difference may be expressed as a time delay difference ΔT, or as a phase (ϕ) difference in radians given by $\phi_{Radians} = 2\pi(\Delta T/T)$. The phase difference in radians can be converted to degrees by $\phi_{Degrees} = (180/\pi) \times \phi_{Radians}$

Choosing one sinusoid as a reference for timing purposes allows the second sinusoid to be expressed as:

$$V_{Sine} = V_p \sin\left(2\pi Ft + \phi_{Radians}\right) \qquad [3.0]$$

The peak level is used to denote the magnitude of the waveform and is the same for both sinusoids shown in the illustration, but may be different distinct values for each sinusoid in other cases. The sinusoid that is chosen as the "***T = 0***" timing reference may be expressed as:

$$V_{Sine-0} = V_{p-Sine-0} \sin\left(2\pi F_{Sine-0}t\right) \qquad [3.1]$$

 Copyright© 2010 Raymond L. Barrett, Jr.

Note the distinction that the value for $\phi_{Radians}$ is zero for the (***0***) reference signal. The magnitude and phase effects of signal processing are contained in the value of V_p and $\phi_{Radians}$ of the sinusoid response.

4.0 Analog Media/Filter/System Response

For the System in Figure 4.0 to be amenable to Classical Analog representation, that system must be causal and Linear, Time-Invariant (***LTI***) to a close approximation. Physical systems are causal in that the inputs always occur before the expected output results occur (i.e., there are no "predictors" in the system). Linearity is assured if the output is proportional to the input and a zero input implies a zero output (at least incrementally). Time-Invariance is assured if the relationship between the output and input changes slowly enough to be inconsequential, such as is caused by drift and aging effects.

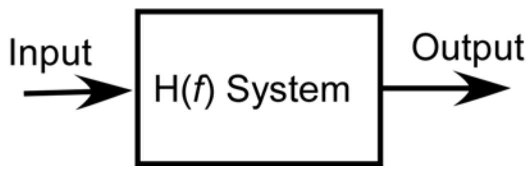

Figure 4.0 A System Diagram with Input and Output Denoted

Such a System is described by a "transfer function" ***H(f)*** that expresses the Output response as a function of the Input stimulus. Other necessary inputs, such as a source of power, are often ignored in simple models.

Several means are commonly used to describe the transfer function, including the "Impulse or Step Response" to describe a response to an impulse or step input respectively. It is not common to design an analog system directly from such a time-domain response, but rather to design with steady-state sinusoidal excitation. To determine the analog system behavior one tool commonly used in the frequency-domain is the Bode plot: it shows the magnitude and phase of the output response with a sinusoidal excitation with a unit magnitude and a zero phase.

Despite the mathematical requirements for a system to be LTI in order to use transfer function descriptions, that rule is often "bent" in describing communications systems because the medium may suffer impairments that are difficult to describe, including time-varying

 Copyright© 2010 Raymond L. Barrett, Jr.

"multipath" interference, and filter structures or media that have significant frequency dependent magnitude and phase delay variations termed "dispersive" effects.

Further, in the process of translating the information from one range of frequencies or bandwidth (BW in Shannon's theorem) to another, we intentionally use nonlinear processes and implementation techniques that are not LTI by definition. One such technique is the use of a multiplication of one waveform by another. Generally, we decompose the signals into sinusoids and represent that function as a multiplication of sinusoids using trigonometric relationships to produce energy at new frequencies, as follows:

$$\sin\alpha\sin\beta = \frac{1}{2}\cos(\alpha-\beta) - \frac{1}{2}\cos(\alpha+\beta) = \frac{1}{2}\cos(\varpi_0 - \varpi_1)t - \frac{1}{2}\cos(\varpi_0 + \varpi_1)t \qquad [4.0]$$

$$\cos\alpha\cos\beta = \frac{1}{2}\cos(\alpha-\beta) + \frac{1}{2}\cos(\alpha+\beta) = \frac{1}{2}\cos(\varpi_0 - \varpi_1)t + \frac{1}{2}\cos(\varpi_0 + \varpi_1)t \qquad [4.1]$$

$$\sin\alpha\cos\beta = \frac{1}{2}\sin(\alpha-\beta) + \frac{1}{2}\sin(\alpha+\beta) = \frac{1}{2}\sin(\varpi_0 - \varpi_1)t + \frac{1}{2}\sin(\varpi_0 + \varpi_1)t \qquad [4.2]$$

5.0 An Analog System Response-

In the following Bode plot, the horizontal frequency axis has the units of Hertz, but could have easily been radians per second as well. The presentation utilizes a logarithmic scaling both for the horizontal frequency axis as well as the vertical response magnitude axis. The vertical axis for the Phase response, however, remains linear in presentation. The two plots are placed in relation to each other so that they can be thought to have a common horizontal axis and each magnitude and phase are related by the corresponding frequency location.

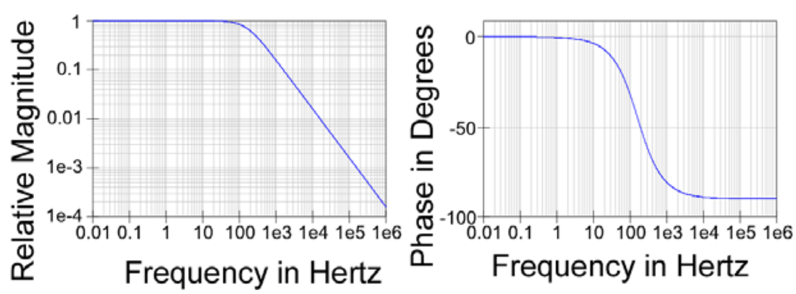

Figure 5.0 Bode Plot of a Single-Pole Low Pass *H(f)* System Response

A system is chosen for discussion that is represented by the Bode plot in Figure 5.0 above. For a steady-state sinusoidal stimulus, the system shows a response pair of magnitude and phase effects plotted versus the excitation frequency. The salient point is 100 Hertz and the behavior indicates the "pole" in the response. Behaviors are significantly different at frequencies above and below the pole frequency.

The frequency axis is plotted logarithmically (as is the Relative Magnitude) because the relationships appear as line segments asymptotically above and below the pole frequency. This system transfer function ***H(f)*** can be represented by the equation:

$$H(f) = \frac{1}{1 + j\left(\dfrac{f}{f_{pole-H}}\right)} = \frac{1}{1 + jF_H} \qquad [5.0]$$

In equation 5.0 the behavior is described as a complex number with the frequency dependence ratio of $F_H = f/f_{pole-H}$ providing the imaginary part. From the single complex number that provides the transfer function at each frequency, we derive the magnitude and phase as:

$$|H(f)| = \frac{1}{\sqrt{1 + F_H^2}} \qquad [5.1]$$

$$\theta_H(f) = -\tan^{-1}(F_H) \qquad [5.2]$$

As the frequency approaches zero (F_H << 1), infinity (F_H >> 1), and also at the pole frequency itself (F_H = 1), we evaluate the transfer function asymptote responses below.

For the case of the stimulus frequency significantly less than the pole frequency:

$$|H(f)|_{F_H \to 0} = \frac{1}{\sqrt{1 + (0)^2}} = 1 \qquad [5.3]$$

$$\theta_H(f)\big|_{F_H \to 0} = -\tan^{-1}(0) = 0 \qquad [5.4]$$

The transfer function magnitude and phase asymptotes agree with the Bode plot of figure 5.0 as the frequency approaches zero, or is significantly less that the 100 Hertz pole frequency.

For the case of the stimulus frequency significantly greater than the pole frequency:

 Copyright© 2010 Raymond L. Barrett, Jr.

$$\left|H(f)\right|_{F_H \to \infty} = \frac{1}{\sqrt{1+(\infty)^2}} = 0 \qquad [5.5]$$

$$\theta_H(f)\big|_{F_H \to \infty} = -\tan^{-1}(\infty) = -90^o \qquad [5.6]$$

The transfer function asymptotes agree with the Bode plot of figure 5.0 as the frequency approaches infinity, or is significantly greater that the100 Hertz pole frequency.

For the case of the stimulus frequency equal to the pole frequency:

$$\left|H(f)\right|_{F_H=1} = \frac{1}{\sqrt{1+(F_H)^2}} = \frac{1}{\sqrt{1+(1)^2}} = \frac{1}{\sqrt{2}} \approx .707 \qquad [5.7]$$

$$\theta_H(f)\big|_{F_H=1} = -\tan^{-1}(F_H) = -\tan^{-1}(1) = -45^o \qquad [5.8]$$

Because the magnitude response depends on the ratio of $\boldsymbol{F_H = f/f_{pole\text{-}H}}$ and for $\boldsymbol{F_H} >> 1$, we can make the approximation:

$$\left|H(f)\right|_{F_H>>1} \approx \frac{1}{\sqrt{(F_H)^2}} = \frac{1}{F_H} \qquad [5.9]$$

The magnitude is inversely proportional to the frequency ratio $\boldsymbol{F_H = f/f_{pole\text{-}H}}$ and for every time the frequency increases by a decade (factor of 10), the magnitude decreases by a decade. On the Bode plot with logarithmic scales, this proportion is shown as the asymptotic straight line above the pole frequency, with a decrease of a decade in magnitude per decade of frequency increase, hence the reason for using the logarithmic axes for the Bode plot magnitude.

The phase response is somewhat different, with symmetrical results around the pole frequency. A series expansion of the $\boldsymbol{tan^{-1}}$ function indicates that it is proportional to the ratio $\boldsymbol{F_H = f/f_{pole\text{-}H}}$ near the pole frequency value, so we simply evaluate the arctangent $\boldsymbol{tan^{-1}}$ at frequencies a decade above and a decade below the pole frequency with the expectation that the errors will be about 10%:

 Copyright© 2010 Raymond L. Barrett, Jr.

$$\theta_H(f)\big|_{F_H\to 10} = -\tan^{-1}(F_H) = -\tan^{-1}(10) = -5.7^o \qquad [5.10]$$

$$\theta_H(f)\big|_{F_H\to 1/10} = -\tan^{-1}(F_H) = -\tan^{-1}(1/10) = -84.3^o \qquad [5.11]$$

The numerical result shows that the ***tan*$^{-1}$** function has nearly reached its asymptotic limits of 0^o and -90^o within the first decade above and below the pole frequency, with a nearly constant slope of -45^o per decade around the pole frequency.

We define the group delay (***GD***) as the slope of the phase function as follows:

$$GD = \frac{d\theta_H(f)}{d\varpi} = -\frac{d\tan^{-1}(F_H)}{d\varpi} = -\frac{1}{1+(F_H)^2}\frac{d(F_H)}{df} = -\frac{1}{2\pi f_{pole-H}}\frac{1}{1+\left(\dfrac{f}{f_{pole-H}}\right)^2} \qquad [5.12]$$

$$GD = -\frac{1}{2\pi}\frac{f_{pole-H}}{f_{pole-H}^2+f^2} \qquad [5.13]$$

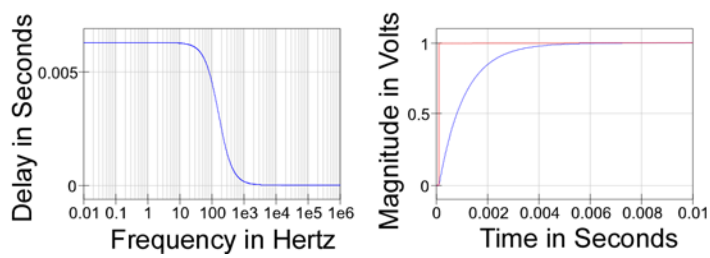

Figure 5.1 Group Delay of *H(f)* System and Step Response

In figure 5.1 above we show the group delay and step response for the 100Hz single-pole system. In figure 5.2 below, we show the tone burst response to a 500Hz tone that is rapidly turned off.

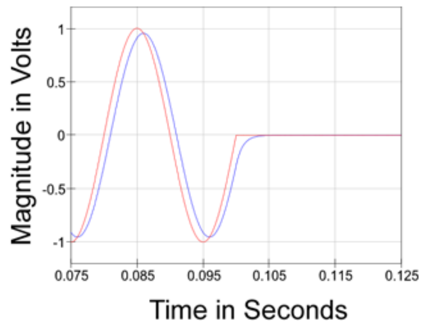

Figure 5.2 Tone Burst Response of *H(f)* System

We see in figure 5.2 above that the single pole lowpass filter has added a delay to the 500 Hz frequency component of the 500 Hz tone burst that is evident as an apparent phase shift. We shall see that the effects of such delays are important issues for frequency and phase synchronization in digital communications over analog channels.

6.0 Sampling Analog Signals to Form Digital Signal Representations

Analog signals are continuous in both time and magnitude, whereas Digital signals are discrete in both time and magnitude. We first convert the Analog signals to a discrete-time representation by sampling and retain the magnitudes as continuous. We then convert the continuous magnitudes to discrete values in a subsequent process, although many contemporary systems do not start from analog representations.

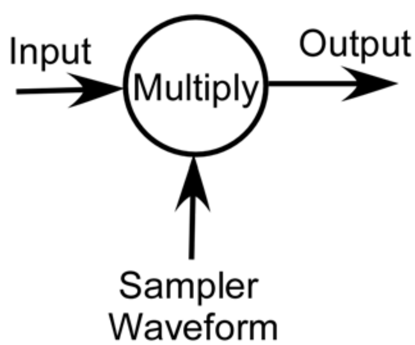

Figure 6.0 Sampling a Continuous-Time Signal

In figure 6.0 above, we perform sampling using the stream of unit magnitude pulses shown in figure 6.1 below in the time domain, as follows:

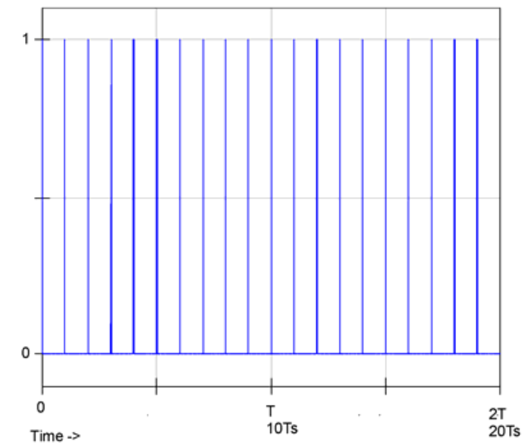

Figure 6.1 Unit Magnitude Periodic Sampling Waveform

As a "practical" discussion matter, we choose a sampling period $\boldsymbol{T_S}$ to be 10x smaller than the period $\boldsymbol{T}$ of the highest frequency "Sine Wave" of interest (i.e., the sampling rate is 10x greater than the highest frequency of interest). The choice is only for illustration.

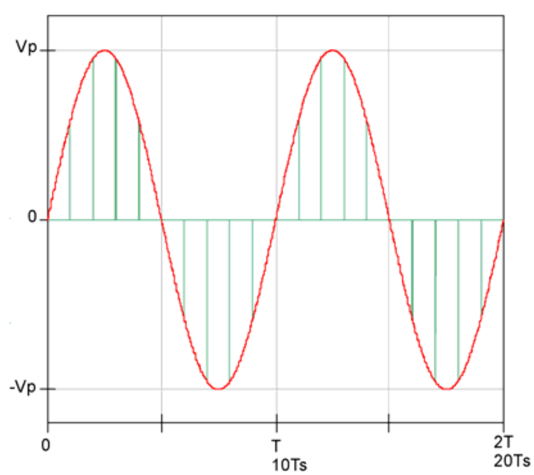

Figure 6.2 Example "Sine Wave" and Sampled Output

Each pulse in the sequence as shown below in figure 6.3, is of a finite, but sufficiently long enough, duration to obtain the sample with accuracy.

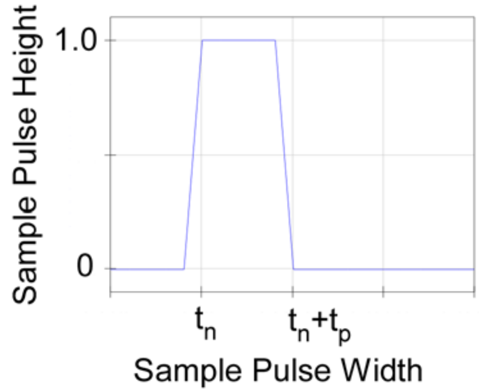

Figure 6.3 A Single Pulse from the Periodic Sampling Waveform

We show in Figure 6.3 above, a single representative pulse with width t_p taken from the sequence of Sampler pulses. The pulse should be as short a duration as can be obtained without sacrificing accuracy. The pulse is shown with a finite rise and fall time to be consistent with a practical sampler device.

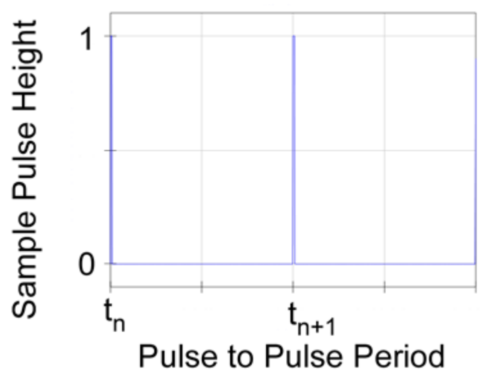

Figure 6.4 A Pair of Adjacent Pulses from the Periodic Sample Waveform

Two adjacent pulses from the periodic Sampler Waveform are shown in Figure 6.4 to illustrate the uniform spacing such that $T_S = (t_{n+1} - t_n)$ for every adjacent interval in the Sampler Waveform.

 Copyright© 2010 Raymond L. Barrett, Jr.

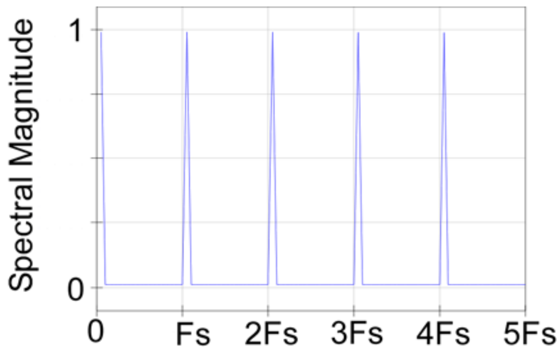

Figure 6.5 A Pair of Adjacent Spectral Lines from the Periodic Sampler Spectrum

As shown in Figure 6.5, the periodic Sampler Waveform exhibits adjacent spectral lines with a frequency spacing $\boldsymbol{F_S}$ related to the sampler period $\boldsymbol{T_S}$ by the relationship $\boldsymbol{F_S} = 1/\ \boldsymbol{T_S}$. The initial spectral line at $\boldsymbol{F_S} = 0$ indicates that the Periodic Sampler can represent DC values correctly.

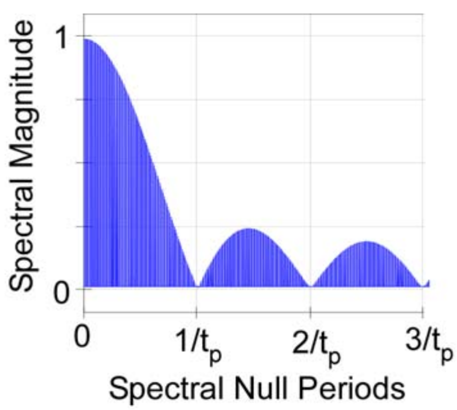

Figure 6.5 Broad Spectral Lines from the Periodic Sampler Spectrum

As illustrated in Figure 6.5, the periodic Sampler Waveform exhibits spectral null behaviors in the frequency domain with spacing $\boldsymbol{F_{Null}}$ as relates to the sampler pulse width and is defined by $\boldsymbol{F_{Null}} = 1/\ \boldsymbol{t_p}$. The spectral line envelope follows a sin(x)/x form with the peak of unity at DC. In other applications, sampling can be used to modulate information to multiple different spectral lines, and is often employed constructively for frequency translation.

7.0 Sampled Analog "Sine Wave" Signals

The frequency spectrum of the "Sine Wave" input shows a single spectral line in Figure 7.0 at the frequency of $F_{SineWave}$:

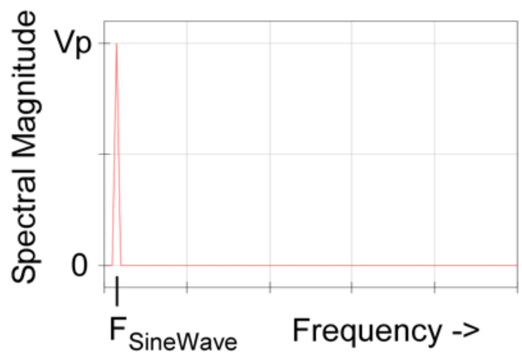

Figure 7.0 Single Spectral Line from the "Sine Wave" Source

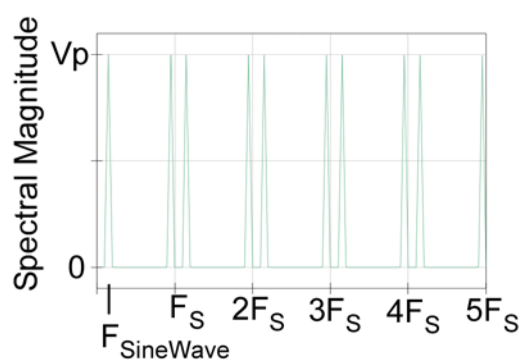

Figure 7.1 Multiple Spectral Lines from the Sampled "Sine Wave" Source

The sampled "Sine Wave" signal consisting of the pulse Output sequence shown in Figure 7.2 with the timing of the sampler but the amplitudes of the "Sine Wave" at the sampling instants is shown in the frequency domain in Figure 7.1; it contrasts with the single "Sine Wave" source spectrum in Figure 7.0 previously shown as the single line. The Sampling waveform "convolves" the "Sine Wave" single line spectrum into spectral line pairs around each multiple of the sampling frequency F_S.

 Copyright© 2010 Raymond L. Barrett, Jr.

The convolution occurs for every spectral line at all multiples of F_S and maintains the sin(x)/x envelope characteristic of the Sampler including the higher frequency parts of the spectrum as Figure 7.2 illustrates:

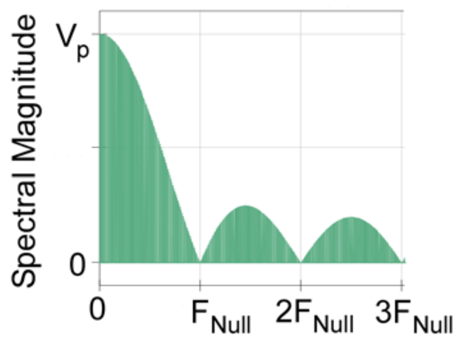

Figure 7.2 Broad Spectral Lines from the Sampled "Sine Wave" Spectrum

An exact reconstruction of the original "Sine Wave" signal is theoretically possible from the sequence of samples, but that possibility is of little practical use because the filter required for reconstruction requires a sin(x)/x impulse response which is non-causal and cannot be realized using an LTI filter.

8.0 Minimum Sampling Frequency for Analog "SineWave" Signals-

To accurately reproduce a "SineWave" Signal, each period of the "SineWave" Waveform must be represented by at least two samples. That means the sampling rate must be higher than twice the highest "SineWave" Signal frequency. One simple way to justify this requirement is to revisit Figure 7.1 and note the spectral line pair around F_S in relation to the spectral line $F_{SineWave}$ from the "SineWave" Waveform itself.

In that part of the spectrum between DC and F_S, two spectral lines appear one at $F_{SineWave}$, and one at (F_S - $F_{SineWave}$). We see that as $F_{SineWave}$ approaches 1/2F_S, the two spectral lines meet midway and are indistinguishable from behaviors with $F_{SineWave}$ above 1/2F_S. The frequency of 1/2F_S is called the Nyquist frequency and the effect of sampling at less than twice that frequency is called "Aliasing." F_S is usually chosen to be significantly higher than the Nyquist rate for any frequencies of interest to avoid Aliasing effects.

 Copyright© 2010 Raymond L. Barrett, Jr.

9.0 Approximate Sampled Analog "Sine Wave" Signals-

If the value of each sample is maintained until the next sample is taken, a "stairstep" approximation of the "Sine Wave" signal results as shown in Figure 9.0 and is labeled as a Zero-Order-Hold (ZOH) response:

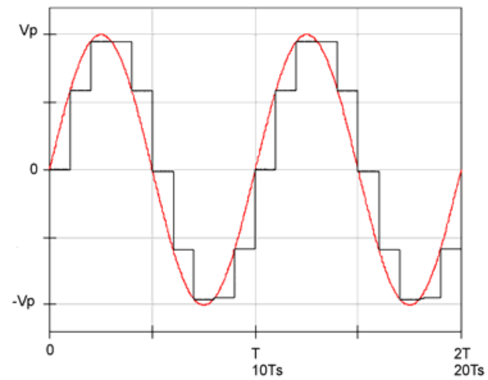

Figure 9.0 Sampled "Sine Wave" with a Zero-Order-Hold Filter Waveform

The Zero-Order-Hold (ZOH) is equivalent to a filter with a pulse response of unit height and pulse width of one sample period T_S, resulting in a causal filter. Unfortunately the causality also introduces a delay of ½ the pulse width or T_S /2 for the entire spectrum.

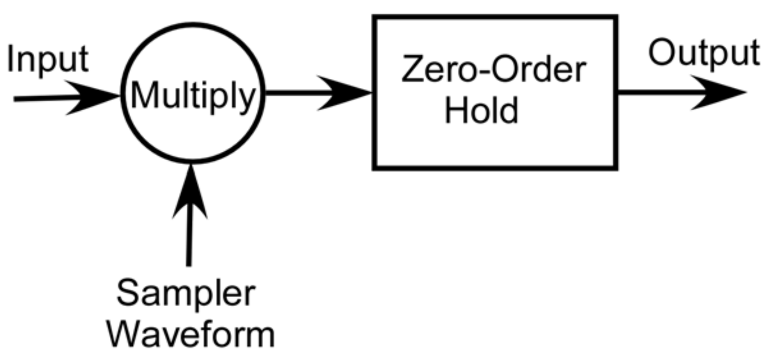

Figure 9.1 Sampler with Zero-Order-Hold Filter System

We show the spectrum in Figure 9.2 of the discrete-time sampled "Sine Wave" signal of Figure 9.0 with the higher-order spectral lines greatly reduced by the ZOH filter.

 Copyright© 2010 Raymond L. Barrett, Jr.

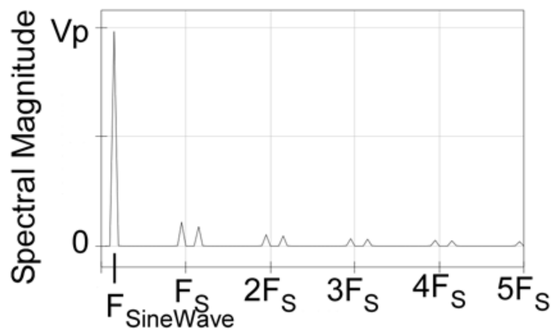

Figure 9.2 Spectrum of the Sampled "Sine Wave" with a Zero-Order-Hold Filter

For Digital Signal Processing (DSP) systems, the signals at the output appear identical to the ZOH waveforms above and consequently have a similar spectral content without ever having been prior analog signals. However, the spectral energy at the multiples of F_S still exists.

10.0 Phase Slope is Group Delay and Visa/Versa

In a duality interpretation of the phase slope, delay of a signal introduces a phase slope. Frequency dependence of delay is known as dispersive delay and causes a waveform envelope distortion and is generally to be avoided or "equalized" to a constant value in communication systems.

Equalization by intentional adding frequency dependent group delay is an analog technique to compensate for group delay and the subject for detail study in itself. Digital Signal Processing (DSP) supports Finite Impulse Response (FIR) filters that inherently provide a constant group delay. However, because the DSP solutions are subject to Nyquist rate limitations they are not employed at some of the higher frequency parts of the spectrum, inductor-capacitor (LC) analog filters with or without equalization are used instead.

11.0 Frequency Translation Using the "Weaver" Modulator Architecture

Signals developed in one part of the spectrum can be translated to another using several means. We choose the "Weaver" architecture for our example because it can be implemented all, or in parts, in both analog and digital forms easily and comparisons are facilitated. The original Weaver architecture was employed to generate and combine "Double Sideband, Suppressed Carrier" signals in two channels with differing phase relationships to produce analog "Single Sideband, Suppressed Carrier" signals. Using single sideband effectively reduced the required bandwidth (BW) for the voice signals at the same power level.

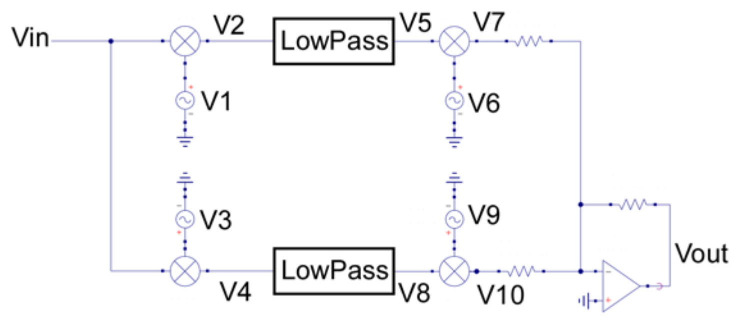

Figure 11.0 "Weaver" Modulator Architecture

The salient features of the Weaver modulator architecture shown in Figure 11.0 above are the use of four waveform sources, four multiplier or mixer structures, two lowpass filters, and a signal combining adder to translate signals from one region of spectrum to another. The waveform sources denoted as $\boldsymbol{V_1}$ and $\boldsymbol{V_3}$ form a quadrature pair at the same reference frequency, but with a 90^{o} phase difference. The waveform sources denoted as $\boldsymbol{V_6}$ and $\boldsymbol{V_9}$ form another quadrature pair at the same reference frequency, not necessarily the same frequency as for $\boldsymbol{V_1}$ and $\boldsymbol{V_3}$ but also with a 90^{o} phase difference. Each channel set is often designated by ***I*** & ***Q*** designators for In-Phase and Quadrature as will become evident. The lowpass filters are often designated in the same fashion for reasons that will also become apparent.

We will develop the entire architecture, although only portions may be implemented in any given design. The Weaver architecture originated circa 1956 with the invention by D. K. Weaver, Jr. of his method of detection and generation of Single-Sideband Signals. His architecture was first described using analog techniques but it has found wide use in digital signal processing for frequency translation applications. We develop the description from the analog technique to enjoy the relative simplicity of the trigonometric relationships and use that reference as the "gold standard" for spectral comparison.

12.0 Analog "Weaver" Modulator

Signals developed from the multiplication of two sinusoids may be expressed algebraically using some combination of the following equations. For each of the relationships below, the angular terms are a sum and a difference in each although the terms differ in the quadrature relationships.

We choose the α argument to be $\omega_0 t$ and the β argument to be $\omega_1 t$ so that the equations may be expressed as:

$$\sin\alpha\sin\beta = \frac{1}{2}\cos(\alpha-\beta) - \frac{1}{2}\cos(\alpha+\beta) = \frac{1}{2}\cos(\varpi_0-\varpi_1)t - \frac{1}{2}\cos(\varpi_0+\varpi_1)t \qquad [12.0]$$

$$\cos\alpha\cos\beta = \frac{1}{2}\cos(\alpha-\beta) + \frac{1}{2}\cos(\alpha+\beta) = \frac{1}{2}\cos(\varpi_0-\varpi_1)t + \frac{1}{2}\cos(\varpi_0+\varpi_1)t \qquad [12.1]$$

$$\sin\alpha\cos\beta = \frac{1}{2}\sin(\alpha-\beta) + \frac{1}{2}\sin(\alpha+\beta) = \frac{1}{2}\sin(\varpi_0-\varpi_1)t + \frac{1}{2}\sin(\varpi_0+\varpi_1)t \qquad [12.2]$$

For each of the relationships above, the angular terms are a sum and a difference in each although the terms differ in the quadrature relationships. Note that neither the ***α,*** nor the ***β*** angles survive, only the sum and differences. We choose the following definitions for the V_{in} signal, V_1 source and V_3 source:

$$V_{in} = A\cos\varpi_0 t \qquad [12.3]$$

$$V_1 = B\cos\varpi_1 t \qquad [12.4]$$

$$V_3 = B\sin\varpi_1 t \qquad [12.5]$$

We can express the V_2 and V_4 products as:

$$V_2 = A\cos\varpi_0 t \bullet B\cos\varpi_1 t = \frac{AB}{2}\cos(\varpi_0-\varpi_1)t + \frac{AB}{2}\cos(\varpi_0+\varpi_1)t \qquad [12.6]$$

$$V_4 = A\cos\varpi_0 t \bullet B\sin\varpi_1 t = \frac{AB}{2}\sin(\varpi_0-\varpi_1)t + \frac{AB}{2}\sin(\varpi_0+\varpi_1)t \qquad [12.7]$$

We position the lowpass filter characteristic frequency so that the difference frequency passes and the sum frequency is rejected with the result that we produce V_5 and V_8 signals:

$$V_5 = \frac{AB}{2}\cos(\varpi_0-\varpi_1)t \qquad [12.8]$$

$$V_8 = \frac{AB}{2}\sin(\varpi_0-\varpi_1)t \qquad [12.9]$$

 Copyright© 2010 Raymond L. Barrett, Jr.

We choose the following definitions for the V_6 source and V_9 source:

$$V_6 = C\cos\varpi_2 t \quad [12.10]$$

$$V_9 = C\sin\varpi_2 t \quad [12.11]$$

We can express the V_7 and V_{10} products as:

$$V_7 = \frac{AB}{2}\cos(\varpi_0 - \varpi_1)t \bullet C\cos\varpi_2 t = \frac{ABC}{4}\cos(\varpi_0 - \varpi_1 - \varpi_2)t + \frac{ABC}{4}\cos(\varpi_0 - \varpi_1 + \varpi_2)t \quad [12.12]$$

$$V_{10} = \frac{AB}{2}\sin(\varpi_0 - \varpi_1)t \bullet C\sin\varpi_2 t = \frac{ABC}{4}\cos(\varpi_0 - \varpi_1 - \varpi_2)t - \frac{ABC}{4}\cos(\varpi_0 - \varpi_1 + \varpi_2)t \quad [12.13]$$

We can express the V_{out} sum as:

$$V_{out} = V_7 + V_{10} = \frac{ABC}{2}\cos(\varpi_0 - \varpi_1 - \varpi_2)t \quad [12.14]$$

The system requirements for the Weaver architecture are met by these equations and a few qualitative points can be made. There are no constraints on the locations of the three frequencies, other that the need to pass the first difference and reject its sum using the lowpass filter. The primary function of the two “channels” in the architecture is to develop the I and Q quadrature relationship between the lowpass filter output signals. The lowpass filters each must pass the difference signal, including any DC components, so they are often referred to as “base band” filtering. The arithmetic differences are “two-sided” and can be thought of as a symmetrical difference around the ω_1 frequency. If an equivalent band-limited signal with the desired spectral content is available, only the final stages are required.

The Weaver architecture, because it reduces the difference to base band, is also known as a “demod-remod” structure, implying a demodulation from one ω_1 carrier frequency to base band, and then a re-modulation onto a new ω_2 carrier frequency. It is important to recognize the trigonometric relationships in the multiplications and the signal frequencies produced. Imperfect balance in the analog implementation implies imperfect cancellation in the summation and the production of unwanted higher frequency output components that are usually removed by filtering.

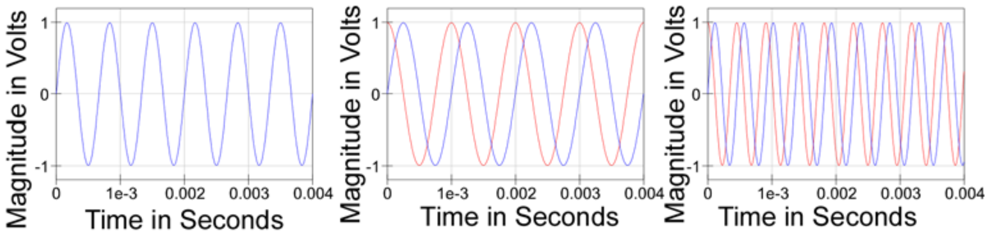

Figure 11.1 V_0 at 1500 Hz, V_1 & V_3 at 1000 Hz, and V_6 & V_9 at 2200 Hz

As illustrated in Figure 11.1 above, we construct the V_{in} signal with a V_0 center frequency at 1500 Hertz. We construct the Weaver modulator with the quadrature sine-wave pairs using the V_1 and V_3 pair in quadrature at 1000 Hz, and the V_6 and V_9 pair in quadrature at 2200 Hz. We have chosen relatively unrelated frequencies to make the spectral content easy to identify, and close enough to discriminate in the spectra. We have chosen relatively low frequencies so that illustrations contain all waveforms near each other in time and frequency.

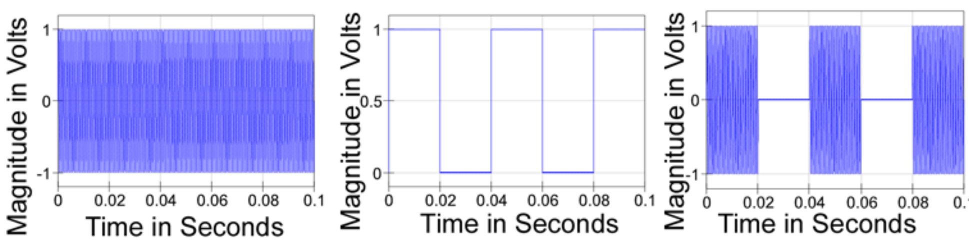

Figure 11.2 V_0 at 1500 Hz, 25 Hz Square Modulation, and V_{in} Tone Burst

As illustrated in Figure 11.2 above, we modify the V_{in} signal with its V_0 center frequency at 1500 Hertz by modulating the 1500 Hz sine wave with a square-wave at 25 Hz to produce the V_{in} tone burst. We employ the particular square-wave tone burst so that the V_{in} spectrum is clearly distinct from the sine-wave sources inside the Weaver modulator.

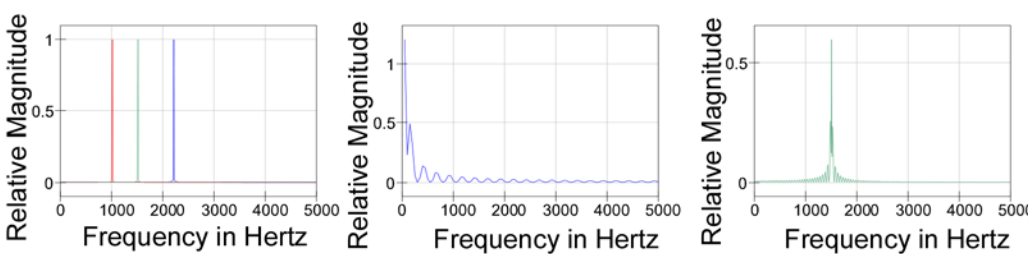

Figure 11.3 V_0, V_3 & V_9 Spectra. 25 Hz Modulation Spectrum, and V_{in} Spectrum

As illustrated in Figure 11.3 above, we see that each sine wave source results in single spectral line at a single frequency, but the square waveform of the modulation has the expected odd-harmonic spectrum multiples of the 25 Hz frequency due to its shape, and that shape produces the side-bands around the carrier in the V_{in} spectrum.

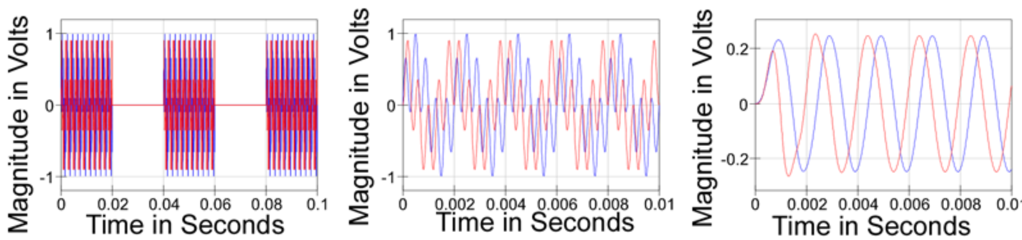

Figure 11.4 V_2 & V_4 Bursts. V_2 & V_4 Burst Detail, and V_5 & V_8 Burst Detail

As illustrated in Figure 11.4 above, we see that the multiplication of the tone-burst modulated V_{in} signal located around 1500 Hz by the V_1 and V_3 pair in quadrature at 1000 Hz, produces similarly shape tone burst results at the corresponding V_2 and V_4 signal locations. As we expect from equations [12.6] and [12.7], the result contains the difference at 500 Hz, and the sum at 2500 Hz, as the detail reveals. Following the lowpass filters, however, the V_5 and V_8 signal locations present only the 500 Hz difference frequency components, and more important, those differences are in quadrature to each other.

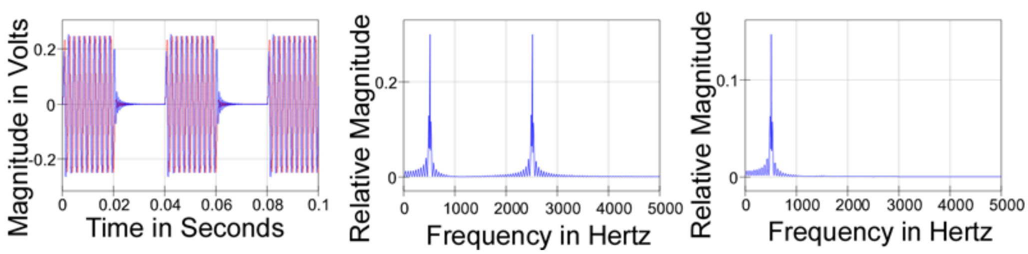

Figure 11.5 V_5 & V_8 Burst. V_2 & V_4 Spectra Detail, and V_5 & V_8 Spectra Detail

As illustrated in Figure 11.5 above, we see that the multiplication of the tone-burst modulated V_{in} signal located around 1500 Hz by the V_1 and V_3 pair in quadrature at 1000 Hz, produces the V_2 and V_4 spectra that contain the difference at 500 Hz, and the sum at 2500 Hz, as the detail reveals. Following the lowpass filters, however, the V_5 and V_8 signal locations present only the 500 Hz difference frequency spectra. The spectra do not reveal the quadrature relationship as found in the time domain traces.

Copyright© 2010 Raymond L. Barrett, Jr.

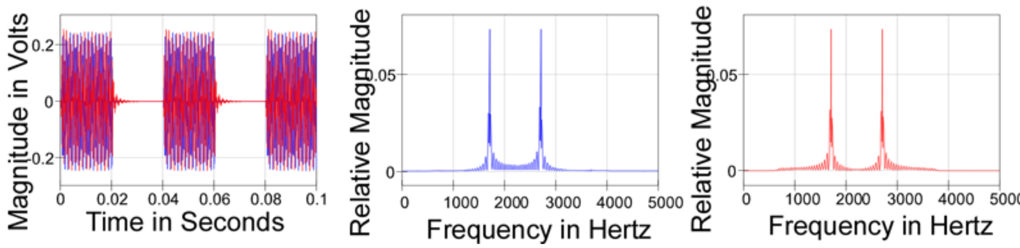

Figure 11.6 V_7 & V_{10} Burst. V_7 Spectra Detail, and V_{10} Spectra Detail

As illustrated in Figure 11.6 above, we see that the multiplication of the 500 Hz frequency tone-burst modulated V_5 and V_8 signals by the V_6 and V_9 pair in quadrature at 2200 Hz, produces the V_7 and V_{10} signals with spectra that contain the difference at 1700 Hz, called the "Lower Sideband," and the V_{out} sum at 2700 Hz, called the "Upper Sideband," as the detail reveals, and we expect from the results of equations [12.12], and [12.13]. Note the lack of any energy at the 2200 Hz carrier frequency, hence the "Double Sideband, Suppressed Carrier" designation.

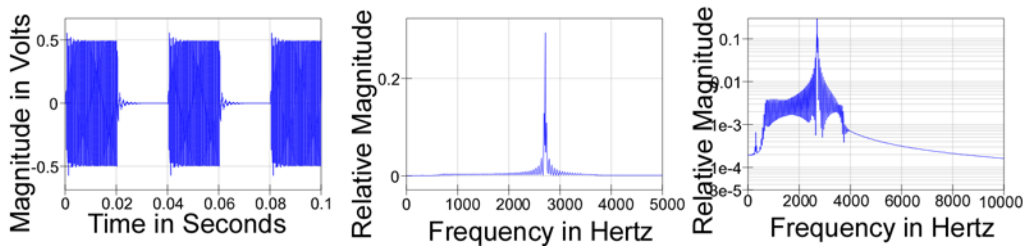

Figure 11.7 V_{out} Burst. V_{out} Spectra, and V_{out} Spectra Logarithmic

Finally, we see the confirmation of equation [12.14] that shows that the Weaver modulator has translated a tone burst signal centered 500 Hz above the V_1 and V_3 quadrature pair at 1000 Hz, to preserve the tone burst modulation to be centered at 2700 Hz, or 500 Hz above the V_6 and V_9 quadrature pair frequency at 2200 Hz. In this implementation, we have produced a "Single Sideband, Suppressed Carrier" signal using the upper sideband. Inverting either the V_7 or V_{10} burst signal prior to the summation would produce the lower sideband as the output.

The Weaver Modulator could be used as easily to translate a 6 MHz wide television channel from near 30 or 40 MHz up to the GHz range, but the illustrations would be more difficult to show together for the purposes of this course.

12.0 Digital "Weaver" Modulator

Signals developed from the multiplication of two sinusoids may be expressed using the continuous analog waveforms as in the previous section, or alternately, each relationship can be satisfied by digital calculations and synthesized using a Digital-to-Analog Converter (DAC) at the output. We have used a sampler and Zero-Order-Hold (ZOH) to simulate the V_6 and V_9 quadrature pair at 2200 Hz. The waveforms have a pronounced "stair step" nature because we have sampled the sine wave signals at 10 kHz, far enough above the Nyquist rate to give an accurate representation and spectrum, but low enough to illustrate the harmonic generation inherent in the digital representation.

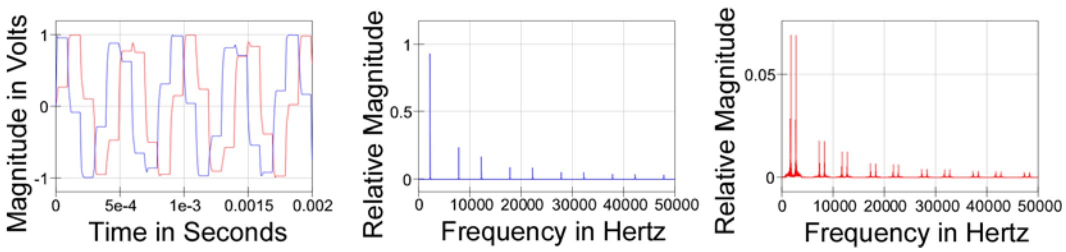

Figure 12.0 V_6 & V_8 Quadrature pair, V_6 & V_8 Spectra, and V_7 & V_{10} Burst Spectra

As illustrated in figure 12.0 above, we see that the ZOH stair-step waveform has considerable energy at the original 2200 Hz but also at odd harmonics above that frequency. Also, in figure 12.0, we see that the multiplication creates the sum and difference signals on either side of the original 2200 Hz but also around the odd harmonics above that frequency.

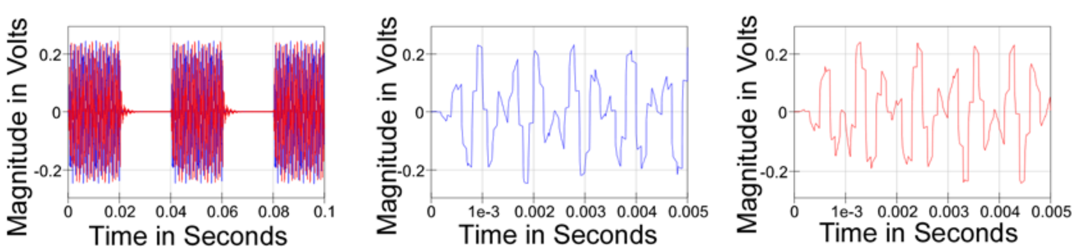

Figure 12.1 V_7 & V_{10} Burst Waveform, V_{10} Burst Detail, and V_7 Burst Detail

In figure 12.1 above, we see that the ZOH stair-step waveform has retained the tone-burst nature of the products, but the details no longer look like very "clean" sums of sine-waves.

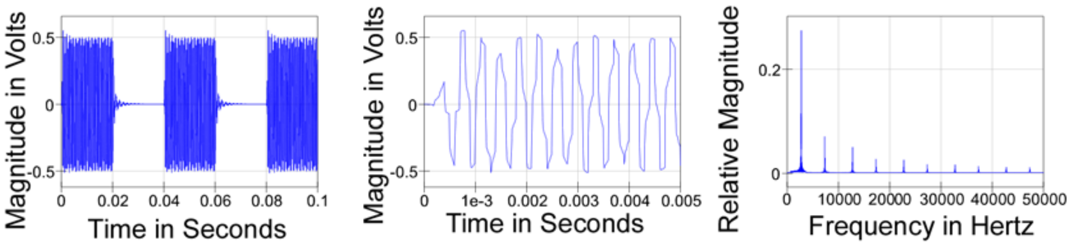

Figure 12.2 V_{out} Burst. V_{out} Burst Detail, and V_{out} Spectra

In figure 12.2 above, we see that the V_{out} summation waveform has retained the tone-burst nature of the products, but this detail does not look like a very “clean” sine-wave tone burst either. The spectrum reveals considerable energy at the harmonics, and intended sum signal has survived the combination of waveforms from the V_7 & V_{10} burst waveforms.

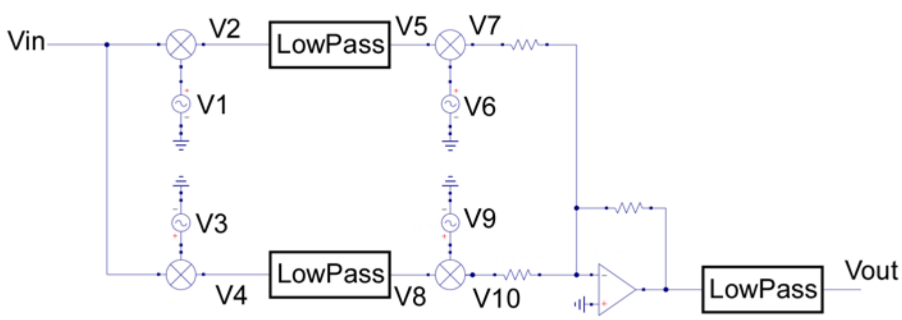

Figure 12.3 Weaver Architecture with Harmonic Suppression Low Pass Filter

We add a lowpass filter to suppress energy at higher frequency harmonics.

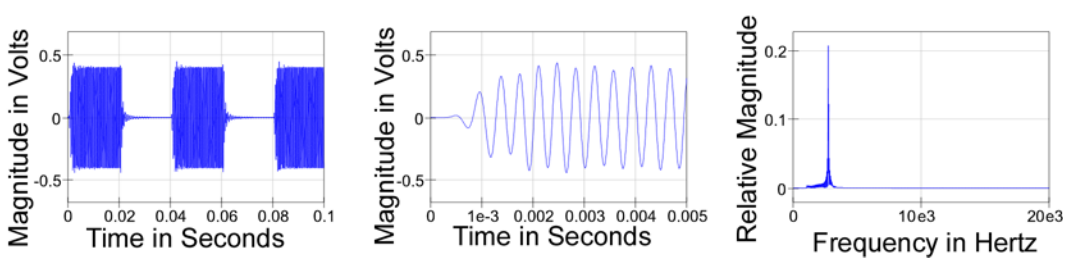

Figure 12.4 Filtered V_{out} Burst. Filtered V_{out} Burst Detail, and Filtered V_{out} Spectra

We see in figure 12.4 above that a lowpass filter can be very effective at removing the energy at the harmonics and the waveform looks much “cleaner” and similar to a sine-wave tone-burst. The remaining artifacts of “ringing” at the leading edge of the tone-burst are amenable to delay equalization of the filter. This can be an important topic for modern digital modulation schemes and inadequate equalization can contribute to bit-error issues. The filter and equalization is also important for analog schemes, too, because the multipliers and other hardware are seldom as ideal as the simulations above would imply.

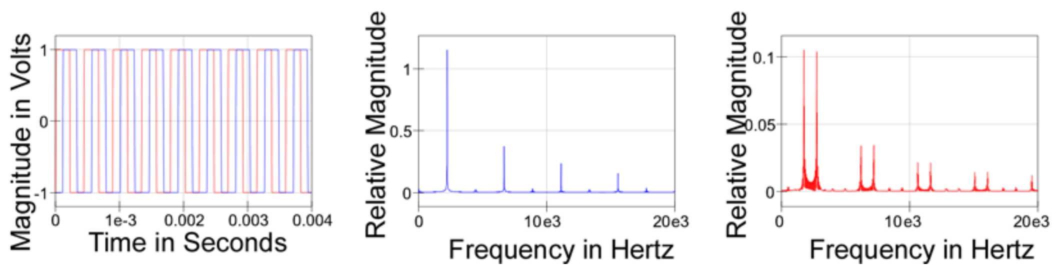

Figure 12.4 V_6 & V_8 Square Wave pair, V_6 & V_8 Spectra, and V_7 & V_{10} Burst Spectra

Insofar as we are using a harmonic suppression filter, and we saw in figure 12.0 that the harmonic energy in the ZOH approximations to a sine wave has no detrimental effects, we illustrate in figure 12.4 an entirely square wave shape and its harmonic structure in relation to the multiplication that creates the sum and difference signals on either side of the fundamental 2200 Hz and also around the harmonics above that frequency.

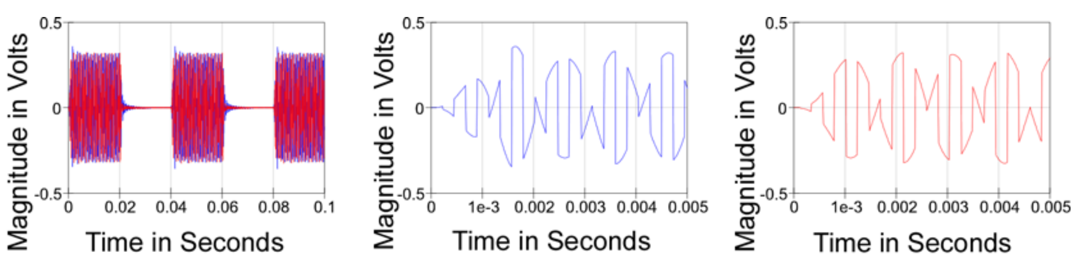

Figure 12.6 V_7 & V_{10} Burst Waveform, V_{10} Burst Detail, and V_7 Burst Detail

In figure 12.6 above, we see that the square waveform has retained the tone-burst nature of the products, but the details look even less like very "clean" sums of sine-waves.

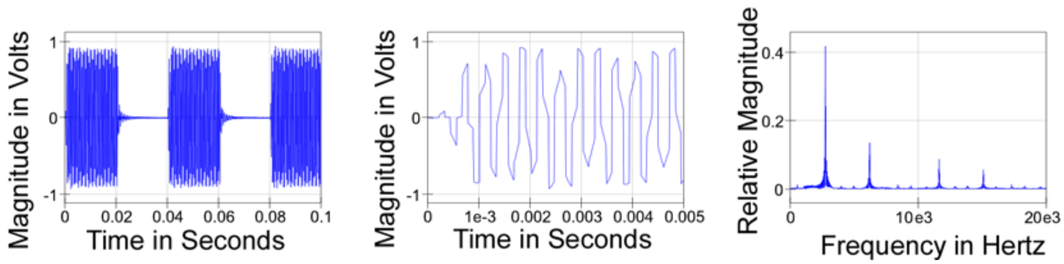

Figure 12.7 V_{out} Burst. V_{out} Burst Detail, and V_{out} Spectra

In figure 12.7 above, we see that the V_{out} waveform has retained the tone-burst nature of the products, but the details again do not look like a very "clean" sine-wave tone burst. The spectrum reveals considerable energy is present at the harmonics, although only the sum signal has survived the combination of waveforms from the V_7 & V_{10} Burst Waveforms.

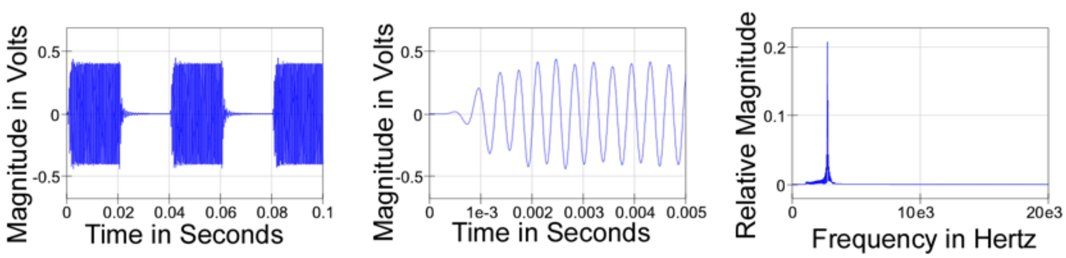

Figure 12.8 Filtered V_{out} Burst. Filtered V_{out} Burst Detail, and Filtered V_{out} Spectra

We see in figure 12.8 above that the harmonic-suppression lowpass filter is still very effective at removing the energy at the harmonics and the waveform looks much "cleaner" and similar to a sine-wave tone-burst. The remaining artifacts of "ringing" at the leading edge of the tone-burst are amenable to delay equalization of the filter.

With the success of using the square-wave at the V_6 and V_8 quadrature pair, we next show the result of employing that same technique at the V_1 and V_3 quadrature pair.

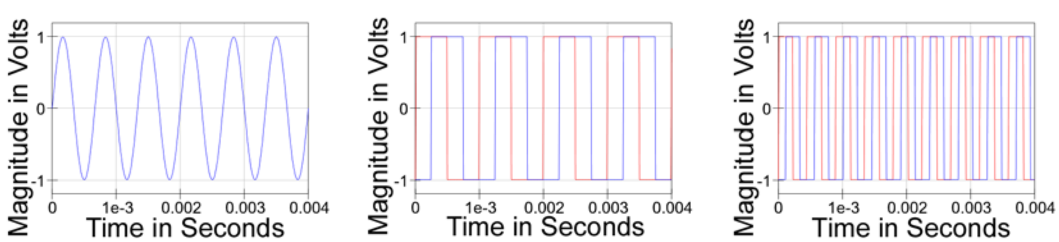

Figure 12.9 V_0 at 1500 Hz, Square V_1 & V_3 1000 Hz, and Square V_6 & V_9 at 2200 Hz

As illustrated in Figure 12.9 above, we keep the V_{in} signal with a V_0 center frequency at 1500 Hertz. But, we construct the Weaver modulator with the two quadrature square-wave pairs with the V_1 and V_3 pair in quadrature at 1000 Hz, and the V_6 and V_9 pair in quadrature at 2200 Hz. We have kept the same frequencies as the sine-wave case for spectral comparison. We have also kept the same presentation organization for ease of comparison. We did not repeat the information of figure 11.2, though, because it is unchanged and the same V_{in} tone burst is retained.

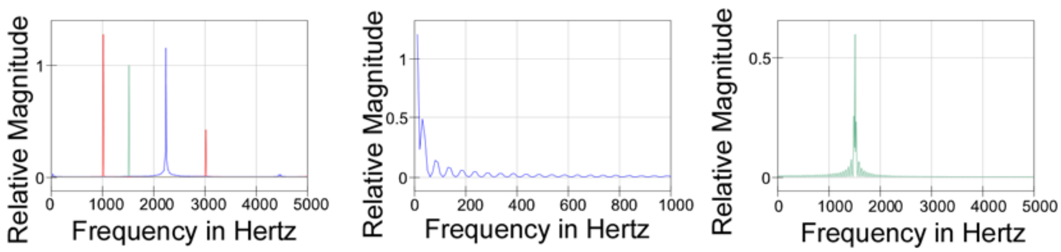

Figure 12.10 V_0, V_3 & V_9 Spectra. 25 Hz Modulation Spectrum, and V_{in} Spectrum

As illustrated in figure 12.10 above and in contrast with figure 11.3 further above, we see that each sine wave source results in single spectral line at a single frequency, but the square waveform of the V_3 signal has a pronounced third harmonic at 3000 Hz. Likewise, some small irregularity in the V_9 signal produces a small output a its second harmonic at 4400 Hz.

The 25 Hz frequency tone burst envelope shape and the spectrum of the V_{in} signal are unchanged with respect to figure 11.3 information.

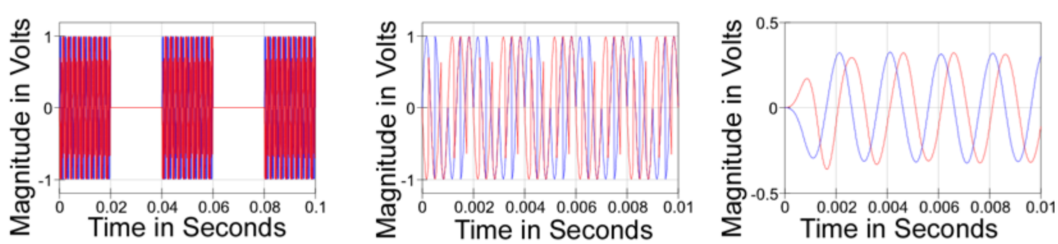

Figure 12.11 V_2 & V_4 Bursts. V_2 & V_4 Burst Detail, and V_5 & V_8 Burst Detail

As illustrated in Figure 12.11 above, we see that the multiplication of the tone-burst modulated V_{in} signal located around 1500 Hz by the V_1 and V_3 pair in quadrature at 1000 Hz, produces similarly shape tone burst results at the corresponding V_2 and V_4 signal locations. As we expect, the result contains the difference at 500 Hz, and the sum at 2500 Hz, as well as harmonics at higher frequencies. In contrast to the sine wave modulation of figure 11.4, we

 Copyright© 2010 Raymond L. Barrett, Jr.

now observe an "envelope" with a square shape. Following the lowpass filters, however, the V_5 and V_8 signal locations present only the 500 Hz difference frequency components, and more important, those differences are in still quadrature to each other. All higher frequency sums and sidebands have been selectively removed.

In comparison to figure 11.5, in figure 12.12 below, the multiplication of the tone-burst modulated V_{in} signal located around 1500 Hz by the V_1 and V_3 pair in quadrature at 1000 Hz, produces the V_2 and V_4 spectra that contain the difference at 500 Hz, and other high-order products that the detail reveals. Following the lowpass filters, however, the V_5 and V_8 signal locations present only the 500 Hz difference frequency spectra. The spectra do not reveal the quadrature relationship as found in the time domain traces, but it is still there.

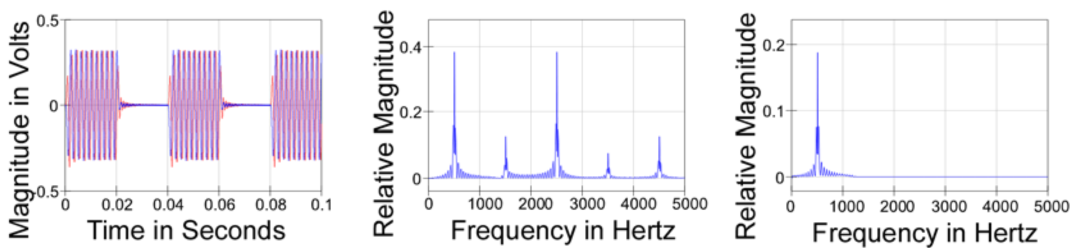

Figure 12.12 V_5 & V_8 Burst. V_2 & V_4 Spectra Detail, and V_5 & V_8 Spectra Detail

We have shown that the important features of the Weaver modulator are retained as the multiplication employs square wave-shapes replacing the sine wave-shape, and laid the foundation for digital implementation.

13.0 Upper and Lower Sidebands

We show the effect of inverting either, or both of the V_5 and V_8 signal magnitudes and the effect on the output signal to further develop the concept of the sidebands.

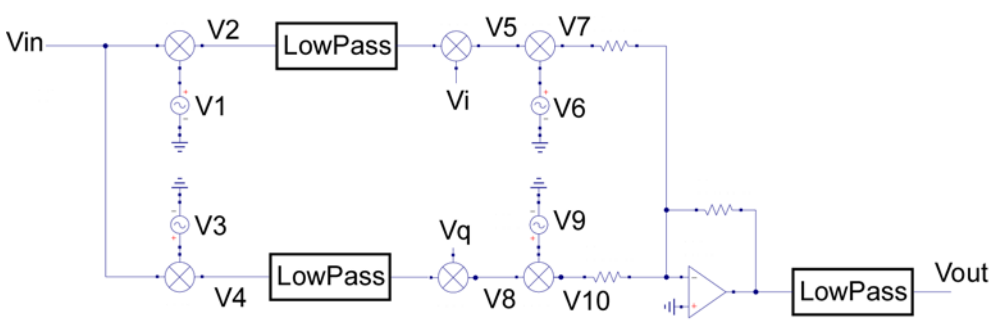

Figure 13.0 Weaver Architecture with V_i and V_q Phase Modulation

In figure 13.0, we insert additional multipliers that are constrained to have a plus or minus 1 magnitude to show the effects on the V_{out} signal, in particular, the development of upper and lower sidebands. With both signals at +1 value, we have all the prior results. There is no effect on prior signals so we examine only the later stage signals.

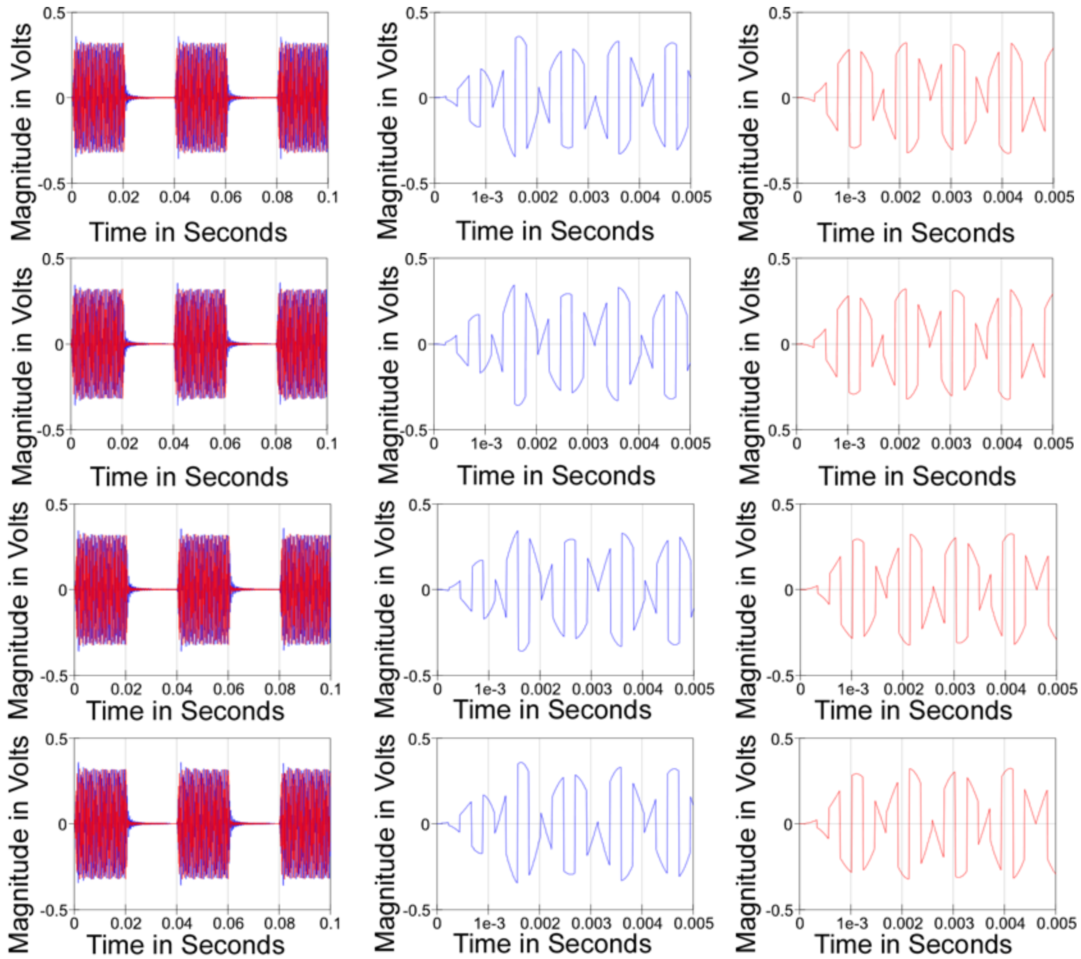

Figure 13.1 V_7 & V_{10} Burst Waveform, V_{10} Burst Detail, and V_7 Burst Detail

In figure 13.1 above, we compare the four cases of the V_7 and V_{10} Burst Waveforms with both V_i and V_q = +1, then V_i = -1 and V_q = +1, then both V_i and V_q = -1, and finally V_i = +1 and V_q = -1, with the noticeable effect of the phase reversals in the burst details.

 Copyright© 2010 Raymond L. Barrett, Jr.

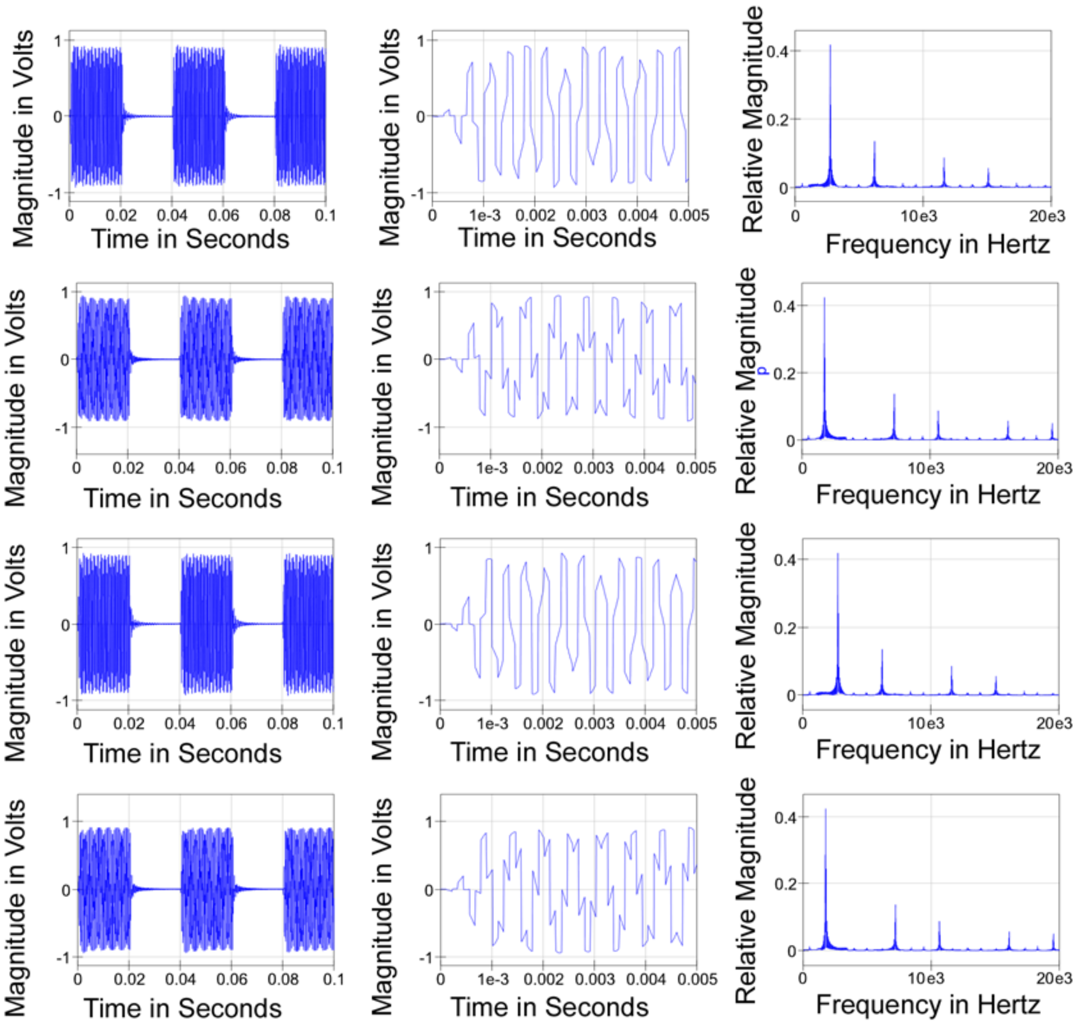

Figure 13.2 V_{out} Burst. V_{out} Burst Detail, and V_{out} Spectra

In figure 13.2 above, we compare the four cases of the V_{out} Burst Waveforms, their detail, and spectra with both V_i and V_q = +1, then V_i = -1 and V_q = +1, then both V_i and V_q = -1, and finally V_i = +1 and V_q = -1, with the noticeable V_{out} wave-shape effect of the phase reversals in the burst details, and the change of spectra. We originally constructed the Weaver modulator so that summation at the output would cancel a difference in frequencies and add the sum of frequencies terms. Each time we alter one phase of the V_7 and V_{10} waveforms, the V_{out} wave-shape is change so that the cancellation changes between sum of frequencies and difference of frequencies. We call the sum of frequencies (2200 Hz + 500 Hz = 2700 Hz) the “upper-sideband,” and the difference of frequencies (2200 Hz - 500 Hz = 1700 Hz) the “lower-sideband,” relative to the V_6 and V_9 quadrature pair frequency at 2200 Hz.

 Copyright© 2010 Raymond L. Barrett, Jr.

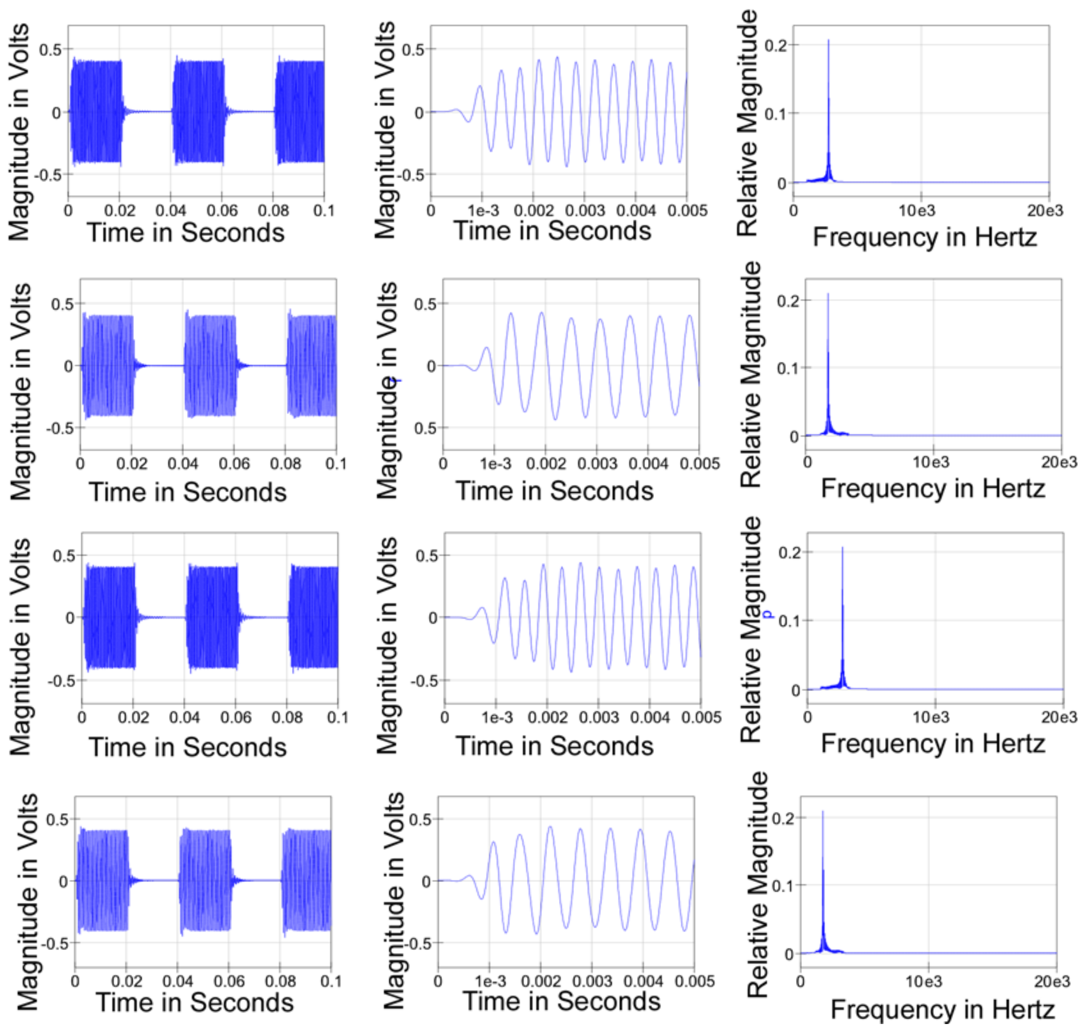

Figure 13.3 Filtered V_{out} Burst. Filtered V_{out} Burst Detail, and Filtered V_{out} Spectra

In figure 13.3 above, we compare the four cases of the V_{out} Burst Waveforms as they appear after filtering by the harmonic suppression lowpass filter, their detail, and spectra with both V_i and V_q = +1, then V_i = -1 and V_q = +1, then both V_i and V_q = -1, and finally V_i = +1 and V_q = -1, with the noticeable V_{out} frequency and phase-reversals. The phase reversals in the burst details reveal that the upper sideband combinations have a 180^o difference between them, as do the lower sideband instances. The change of spectra shows only the frequencies related to the upper or lower sideband productions, but no information about the phase.. We originally constructed the Weaver modulator so that summation at the output would cancel a difference in frequencies and add the sum of frequencies terms.

14.0 Retrieving the Information from the Modulation Output

We recover the information from the V_{out} signal using another receiving Weaver modulator in a mirror image to the one that generated the V_{out} signals. We connect the previously discussed V_{out} signal with an appropriate "Channel" to the input of the receiving Weaver modulator. The channel may be a cable connection, an RF connection, or an optical connection so long as the channel preserves the wave shapes.

One important feature of the receiving Weaver modulator is the interchange of the quadrature pairs. All corresponding signals in the receiving Weaver modulator are denoted with the VN' designation and have the same relative positions as in the transmitting Weaver modulator, except for the interchange of quadrature pairs, as shown in figure 14.0 below.

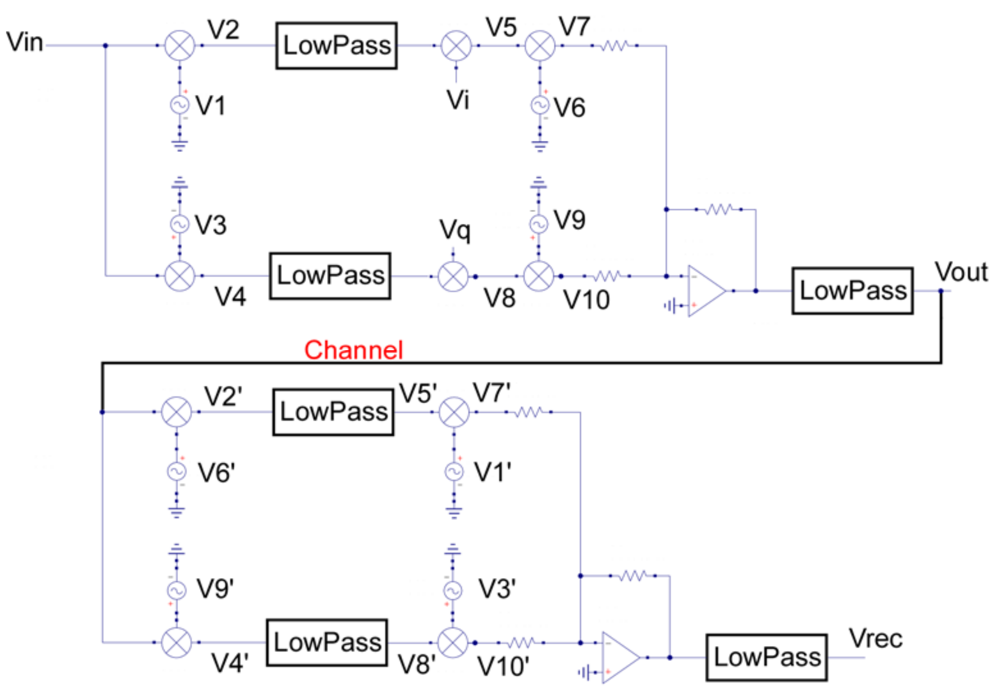

Figure 14.0 Communicating Interconnection of Weaver Modulators

We directly connect the channel to the input of the receiving Weaver modulator and use the V'_6 & V'_9 quadrature pair at 2200Hz to produce a 500 Hz difference. The 500 Hz difference is assured because the channel always has either the 1700 Hz lower sideband or the 2700 Hz upper sideband and a difference will always contain the 500 Hz, regardless of where the sum signal may be. The sum is irrelevant because the low pass filters remove it. Below in figure

 Copyright© 2010 Raymond L. Barrett, Jr.

14.1, we see the channel tone burst and a detail of the V'_2 and V'_4 signals that result, as well as the spectrum of the result.

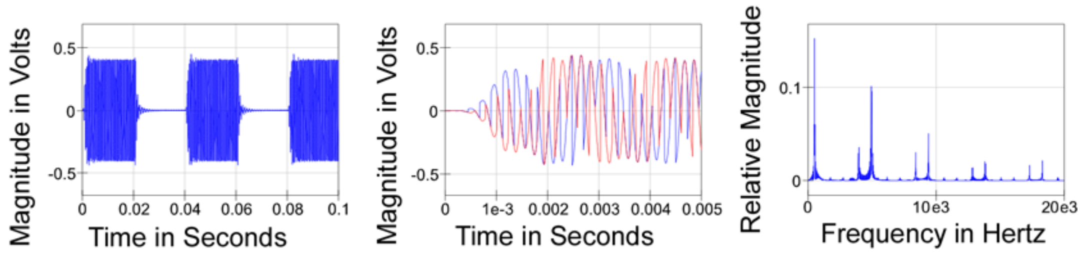

Figure 14.1 ***Channel*** **Burst. V'_2 & V'_4 Burst Detail, and V'_2 & V'_4 Spectra Detail**

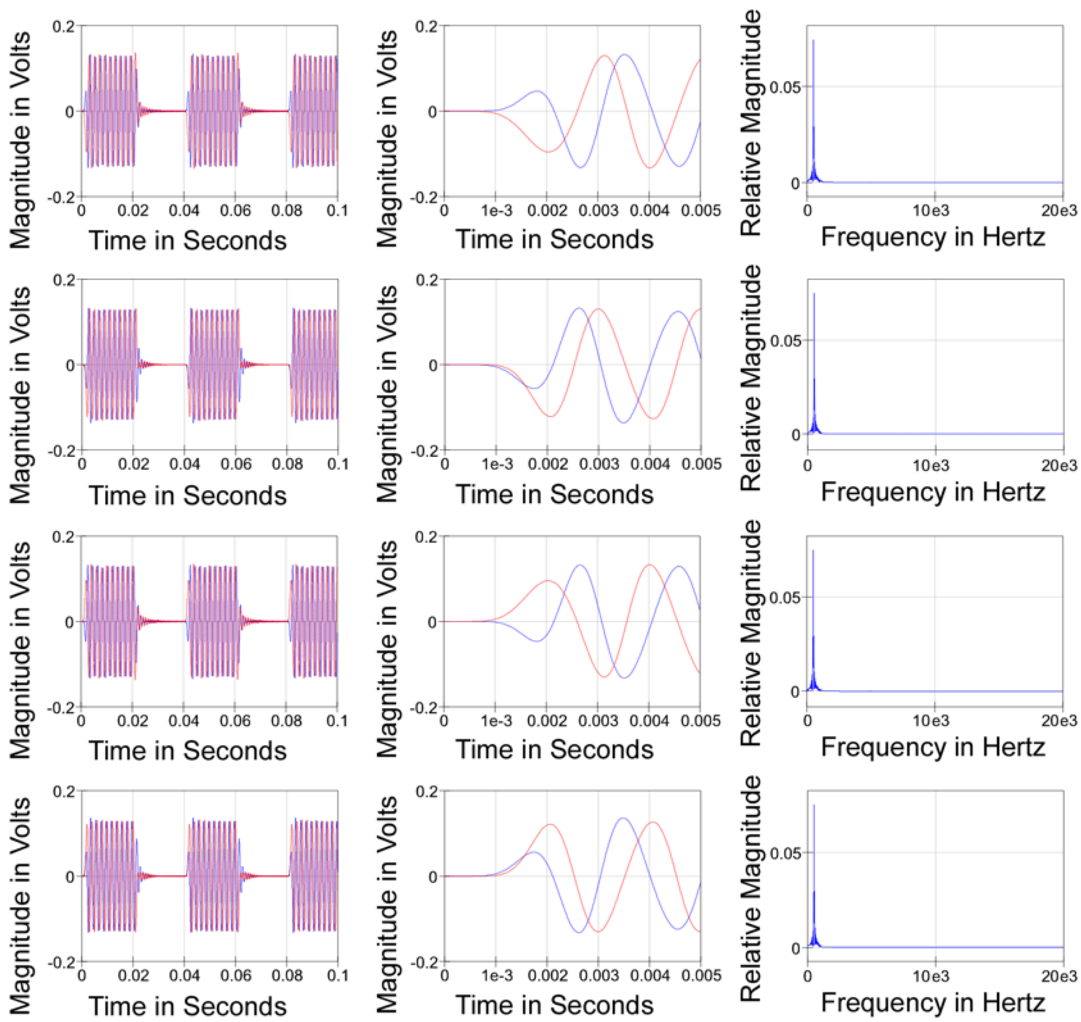

Figure 14.2 V'_2 & V'_4 Burst. V'_2 & V'_4 Burst Detail, and V'_2 & V'_4 Spectra Detail

In figure 14.2 above, we see all four combinations of multiplications applied to the transmitting Weaver modulator and the phase relationships of the 500 Hz V'_2 and V'_4 signals.

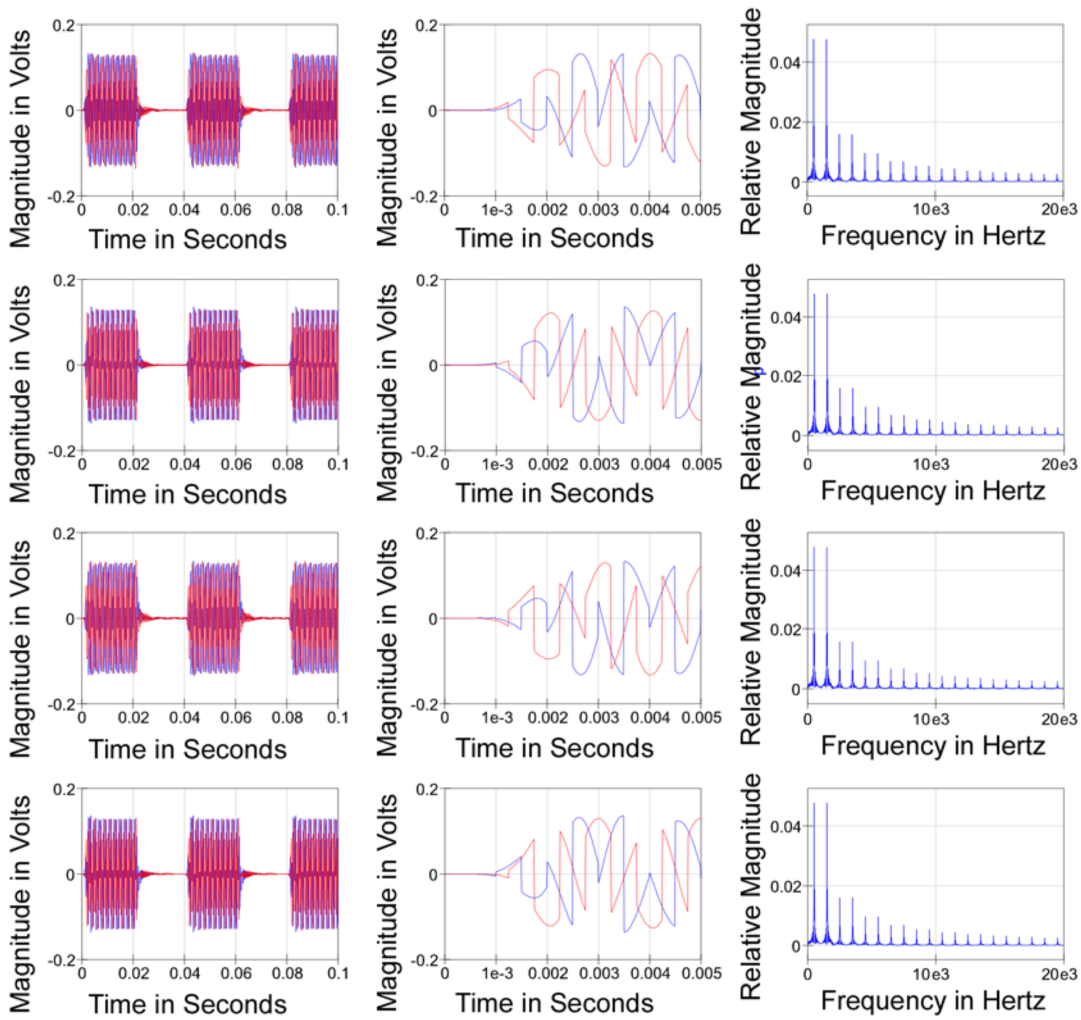

Figure 14.3 V'_7 & V'_{10} Burst. V'_7 & V'_{10} Burst Detail, and V'_7 & V'_{10} Spectra

In figure 14.3 above, we see all four combinations of the V'_2 and V'_4 signals and the products produced at the V'_7 and V'_{10} multiplier outputs. The spectra are identical in appearance because they differ only in the relative phase of the harmonics of the V'_7 and V'_{10} multiplier outputs.

 Copyright© 2010 Raymond L. Barrett, Jr.

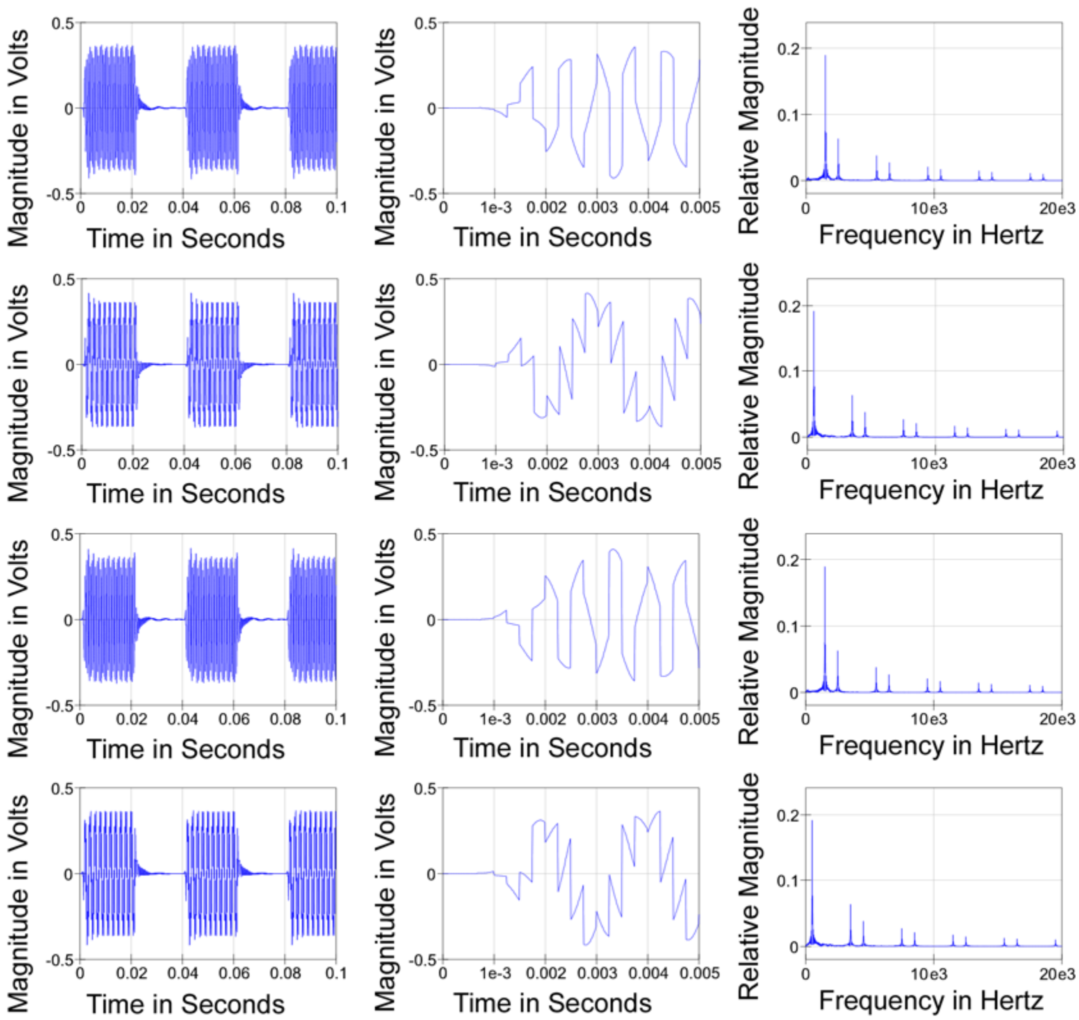

Figure 14.4 Sum Burst. Sum Burst Detail, and Sum Spectra

In figure 14.4 above, we see all four combinations of the *V'$_7$* and *V'$_{10}$* multiplier output signals summed together to cancel either the upper or lower sideband components.. The spectra reveal that the summation produces the sum of 500 Hz plus 1000 Hz to produce the original 1500 Hz tone burst, or a difference is produced between 500 Hz and 1000 Hz to produce a 500 Hz tone burst. Further, the two 1500 Hz cases are 180^{o} degrees relative to each other, as are the two 500 Hz cases.

 Copyright© 2010 Raymond L. Barrett, Jr.

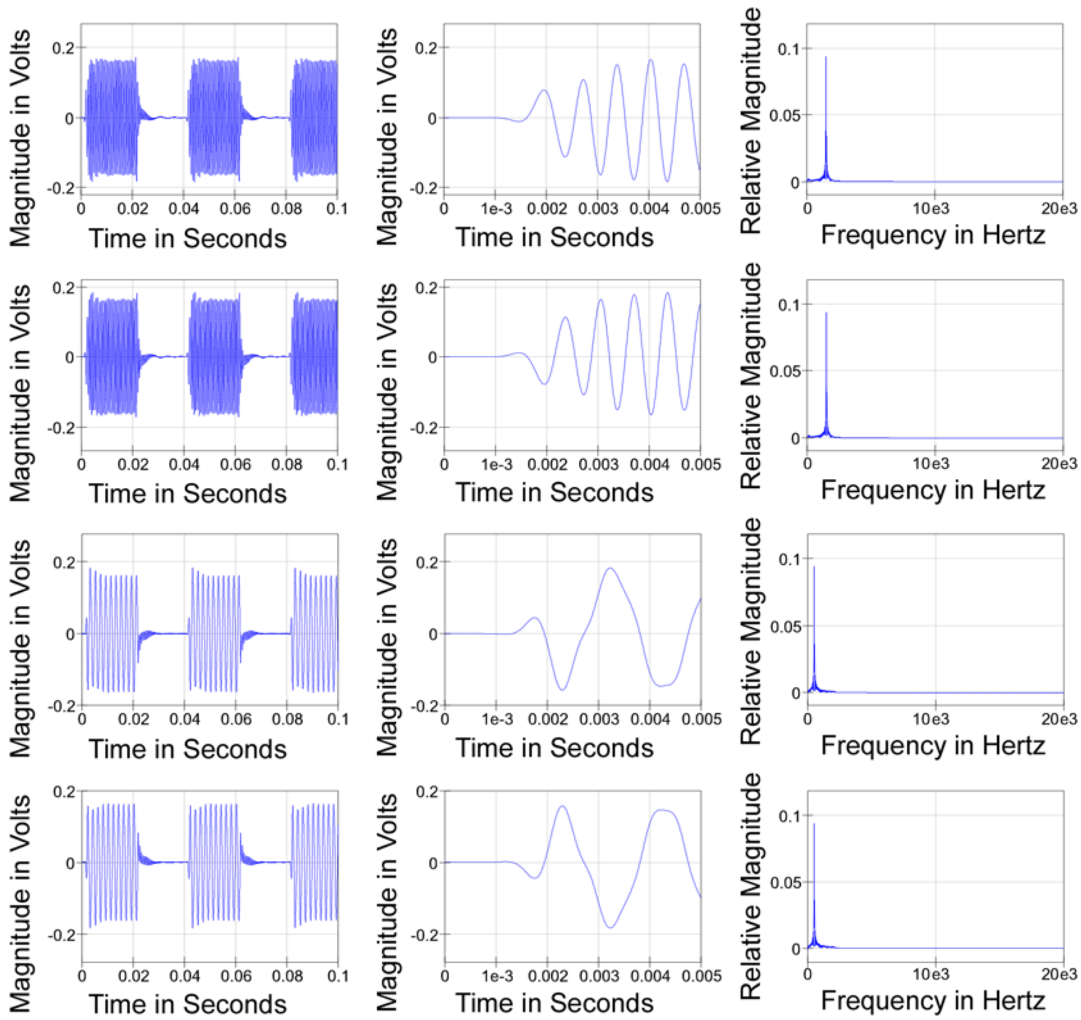

Figure 14.5 Filtered Receive Burst. Burst Detail, and Filtered Spectra

In figure 14.5 above, we again see all four combinations of the summations that produce the sum of 500 Hz plus 1000 Hz to produce the original 1500 Hz tone burst, or difference is produced between 500 Hz and 1000 Hz to produce a 500 Hz tone burst, but with higher harmonics removed. Further, the two 1500 Hz cases are 180^{o} degrees relative to each other, as are the two 500 Hz cases in a much more obvious presentation.

In all cases, the tone-burst nature of the modulation presented at $\boldsymbol{V_{in}}$ to the transmitting Weaver modulator has been retained in a scale representation.

15.0 Reduction of the Weaver Modulator Scheme to Carry Amplitude and Phase Data
We recognize that we have introduced two phase-inverting multipliers following the transmitting Weaver modulator's lowpass filter. We can utilize those two signals to represent two independent bits of information. Further, because we have shown that the on/off nature of the tone burst has been preserved, we will also use amplitude variations to carry additional bits of information.

First, let us re-introduce the transmission of the phase-modulated signals in a modification to the Weaver architecture.

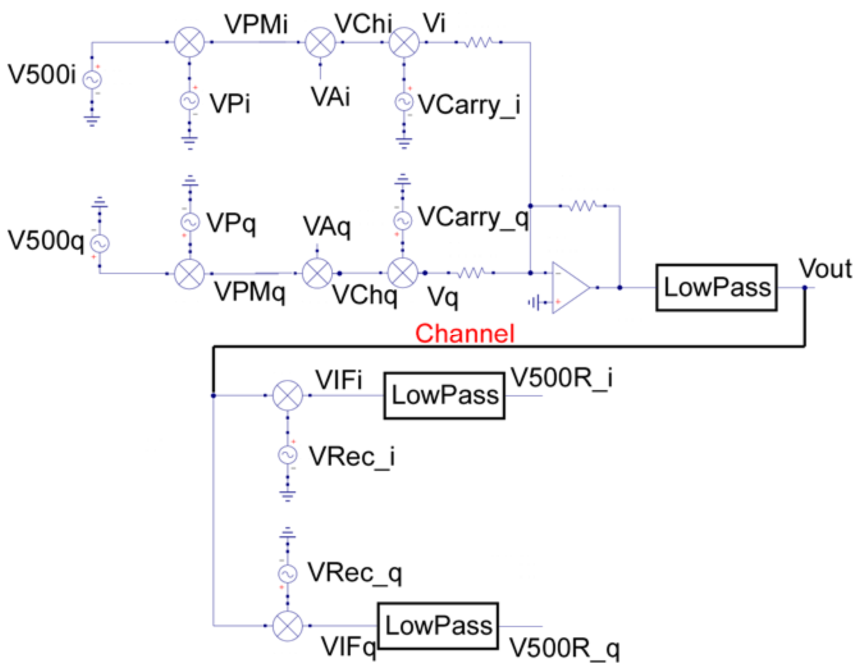

Figure 15.0 Weaver Modulator Modified to Carry Amplitude and Phase Data

In figure 15.0 above, we generate a quadrature pair of sine wave signals at 500 Hz directly and designate them as ***V500i*** and ***V500q*** above. We introduce a pair of multiplying phase modulation signals as shown as ***VPi*** and ***VPq*** in figure 15.1 below. We constrain the signals to allow polarity changes at 10 msec intervals but otherwise show either polarity during any 10 msec period. The sequences we have chosen are distinct for illustration purposes and can be considered the sign bit of a sign/magnitude digital sequence.

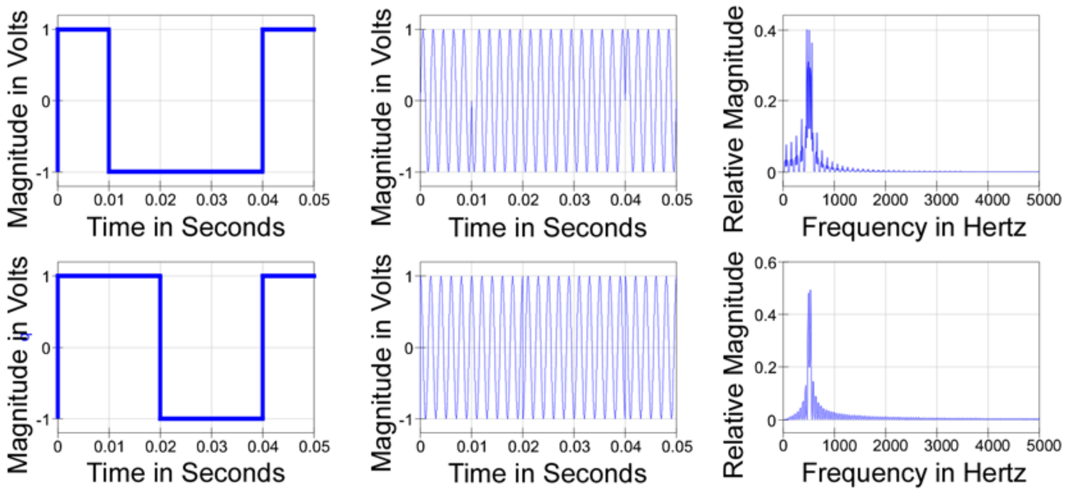

Figure 15.1 The VPi and VPq Sequences, the VPMi and VPMq Signals, and Spectra

In figure 15.1 above, the ***VPi*** and ***VPq*** sequences produce 180^o phase shift in the ***V500i*** and ***V500q*** sine wave 500 Hz quadrature pair. The "Bi-Phase" result for each signal introduces the sidebands around the 500 Hz carrier from each modulating sequence as shown in the spectra. No higher harmonics are produced, and no DC component is added to the signal by the phase modulation. Effectively, we have one bit of data in each pattern every 10 msec.

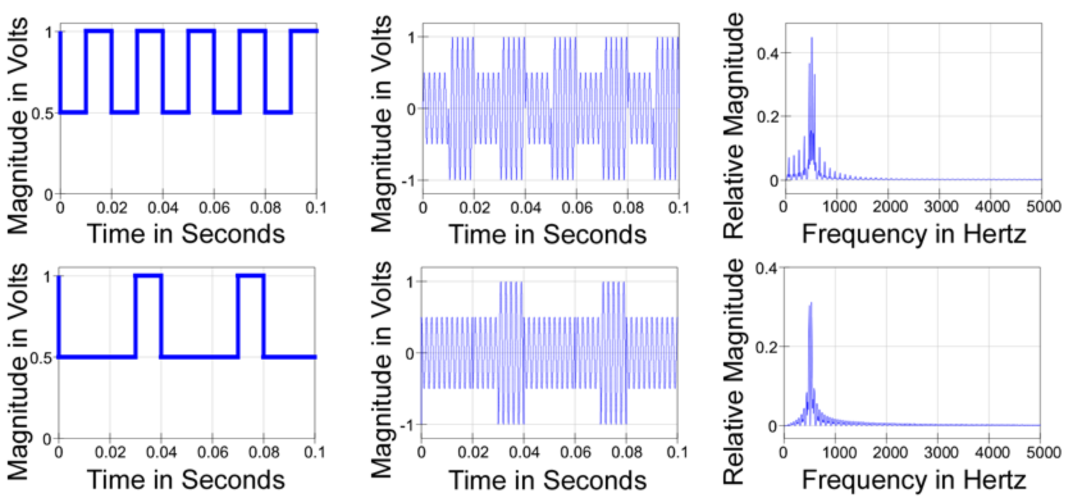

Figure 15.2 The VAi and VAq Sequences, the VChi and VChq Signals, and Spectra

In figure 15.2 above, the ***VAi*** and ***VAq*** sequences produce attenuation of the ***VPMi*** and ***VPMq*** signals effectively amplitude modulating each. The further amplitude modulation of the already phase modulated 500 Hz signals further modifies the sidebands around the 500

 Copyright© 2010 Raymond L. Barrett, Jr.

Hz carrier with each new modulating sequence as shown in the spectra. No higher harmonics are produced, and no DC component is added to the signal by the amplitude modulation, but the changes in the amplitude of the ***VChi*** and ***VChq*** signals are easily associated with the controlling attenuation bit patterns.

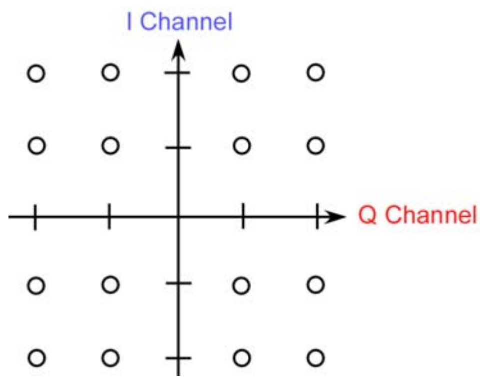

Figure 15.3 The I Channel and Q Channel Bit Constellation

The addition of the two attenuation bits per symbol to the existing two phase modulation bits makes the pattern a 4-bit symbol corresponding to the 16 locations on the "Constellation" as shown in figure 15.3 above. The phase modulation corresponds to the sign bit of the axis associated with each location in the constellation, and the attenuation with the displacement along that axis. With 16 states, the pattern is known as a 16-QAM pattern. More bits can be added to the attenuator by creating more steps and 256-QAM to 1024-QAM are in use in channels with a Signal-to-Noise Ratio (SNR) that permits recovery of the data.

Using the 10 msec data interval we have employed in the example, the "symbol rate" is 100 baud, and with 4 bits per symbol, the bit rate is now 400 bits/second. Increasing the number of steps of amplitude modulation employed increases the bit rate but retains the 100 baud symbol rate.

The constellation can be mapped using the ***VChi*** and ***VChq*** signals, or anywhere in the structure that *I* and *Q* channel information is distinct.

After quadrature modulation onto a single carrier frequency as shown in figure 15.3 below, the signal is raised to the frequency appropriate for the transmit/receive channel and only further requires summation of the two independent double sideband suppressed carrier signals into a single signal.

 Copyright© 2010 Raymond L. Barrett, Jr.

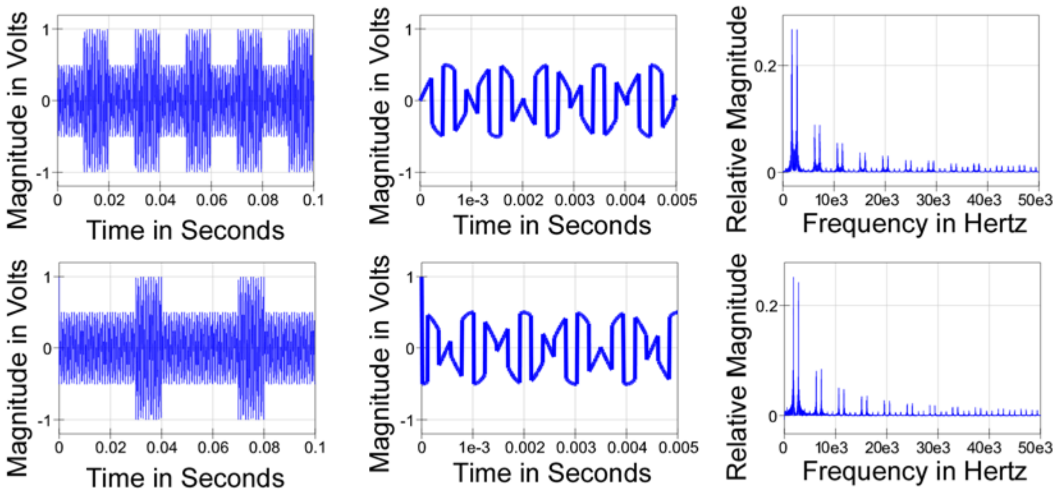

Figure 15.3 The Vi and Vq Signals, Vi and Vq Signal Details, and Vi and Vq Spectra

In figure 15.3 above, the ***VCHi*** and ***VChq*** signals are multiplied by the 2200 Hz quadrature ***VCarry_i*** and ***VCarry_q*** square wave signals to produce the ***Vi*** and ***Vq*** signal pair**.** We note that there is a pair of sidebands around the 2200 Hz carrier frequency, as well as many of its harmonics. In a later detail, we shall see that the pairs are centered at 2200 +/- 500 Hz, or 1700 Hz and 2700 Hz, but neither contributes any signal at the 2200 Hz carrier frequency, or near DC.

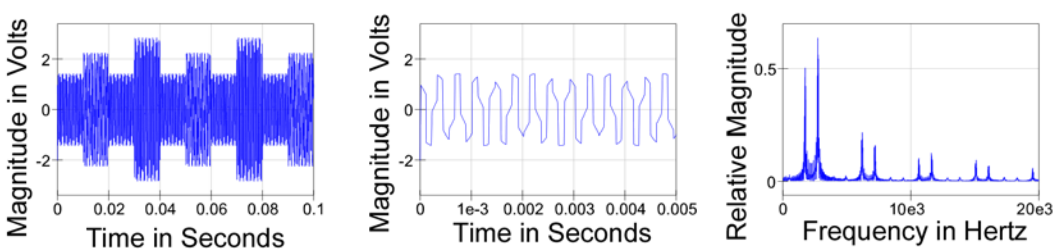

Figure 15.4 The Sum of Vi and Vq Signals, The Sum Signal Details, and Spectrum

In figure 15.4 above, the summation of ***Vi*** and ***Vq*** signals produces a signal with an amplitude modulation pattern that does not clearly reveal either of the component patterns, but is a form of composite with more levels of amplitude variation than either pattern alone. The phase modulation patterns are not easily discerned either. However, the higher order harmonics are present and are removed by the lowpass filter as shown below in figure 15.5, before becoming the ***Vout*** signal presented to the communications channel.

 Copyright© 2010 Raymond L. Barrett, Jr.

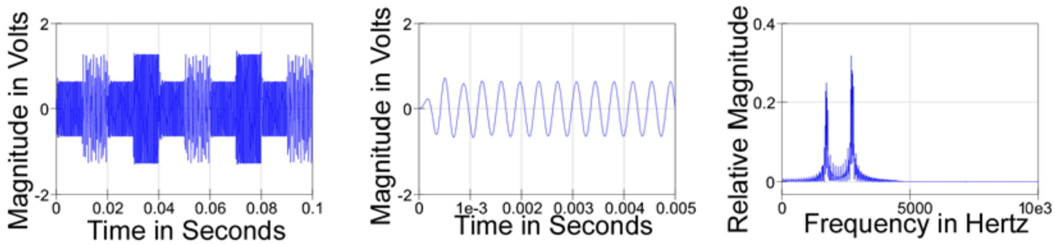

Figure 15.5 The Vout Filtered Signal, The Signal Detail, and its Spectrum

In figure 15.5 above, the filtered ***Vout*** signal shows the two sidebands around the 2200 Hz carrier frequency at 1700 Hz and 2700 Hz with no higher or DC signals present. Further, there is no signal at the 2200 Hz carrier frequency so the QAM signal is called a Double-Sideband, Suppressed Carrier signal. Such a signal, at an appropriate carrier frequency other than 2200 Hz could be used for an RF channel, or a cable/wire channel.

16.0 Reduction of the Weaver Modulator Scheme to Receive Amplitude and Phase Data

We have produced a signal in the channel using the modified Weaver architecture above and now use another modified Weaver modulator shown in figure 16.0 below to retrieve the modulated signal patterns so that the original data sequence can be reconstructed.

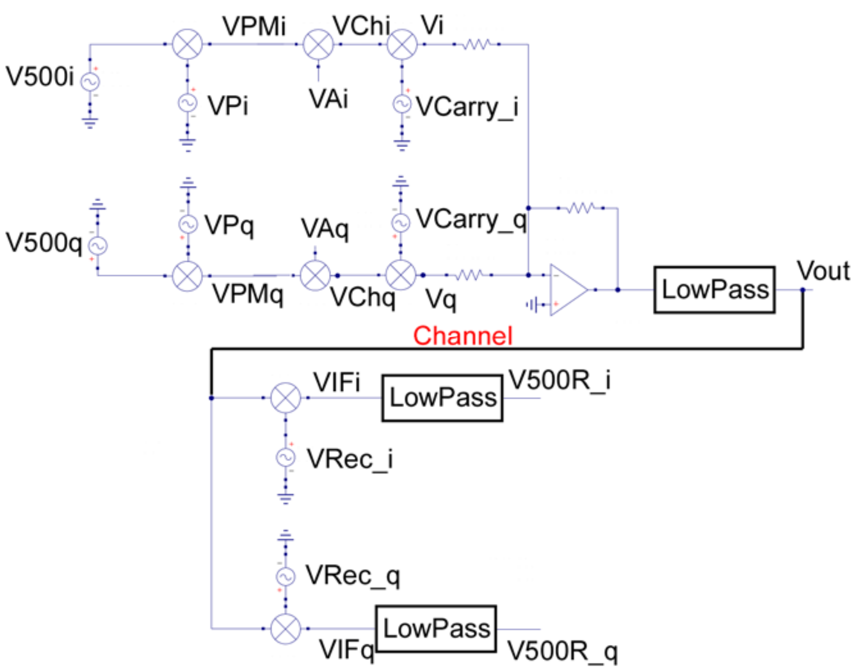

Figure 16.0 Weaver Modulator Modified to Receive Amplitude and Phase Data

The structure we employ is straightforward, but we shall see that there are a few issues in synchronizing the receiving Weaver modulator, as well as uncertainties in channel identification and phase polarities

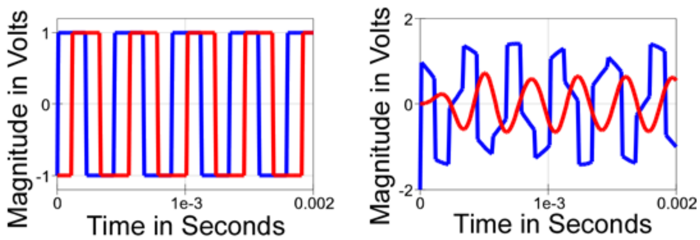

Figure 16.1 *VCarry_i* and *VCarry_q* Square Waves, Filtered and Un-Filtered Vout

In figure 16.1 above, we show the square wave signals that were used to produce the components of the ***Vout*** signal, as well as the filtered ***Vout*** signal. The unfiltered ***Vout*** signal exhibits edges that are synchronized with the edges of the square waves, but the filtered ***Vout*** shows a time/phase shift that is an artifact of the filtering used to reduce the harmonic content of ***Vout***. We have employed an analog filter, but a digital filter too, will introduce delays.

We have simulated the receive Weaver modulator with a quadrature pair of square wave sources at ***VRec_I*** and ***VRec_q*** that are identical to those used in the transmitter for ***VCarry_i*** and ***VCarry_q*** recognizing that we will have some issues. At this point, the usage is intentional so that we can illustrate the problem and discuss the solution

Recall that the signal in the channel is: "a Double-Sideband, Suppressed Carrier signal." We have no direct means to synchronize a remote receiver to the correct ***VCarry_i*** and ***VCarry_q*** frequency , nor to the required phase relationships. We require an external carrier recovery means to produce the ***VRec_I*** and ***VRec_q*** signals at the correct frequency and phase for optimal data recovery.

We illustrate below that we can develop such a signal from the channel signal itself. First, we discuss the mixing of the channel signal with itself by a square-law rule. Below in figure 16.2, we show the algebraic square of the ***Vout*** signal. Combining signals A plus B and squaring follows the simple rule:

$$(A+B)^2 = A^2 + 2AB + B^2 \qquad [16.1]$$

with:

$$A = V_{1700}\cos(2\pi \bullet 1700 + \theta_{1700}) \qquad [16.2]$$

 Copyright© 2010 Raymond L. Barrett, Jr.

$$B = V_{2700}\cos(2\pi \bullet 2700 + \theta_{2700}) \qquad [16.3]$$

The stage is set for producing sum and difference terms from the AB product, as well as DC terms and twice frequency terms. We see below in figure 16.2 that we have energy at 3400 Hz, 4400 Hz, and 5400Hz, as well as the lower frequency terms.

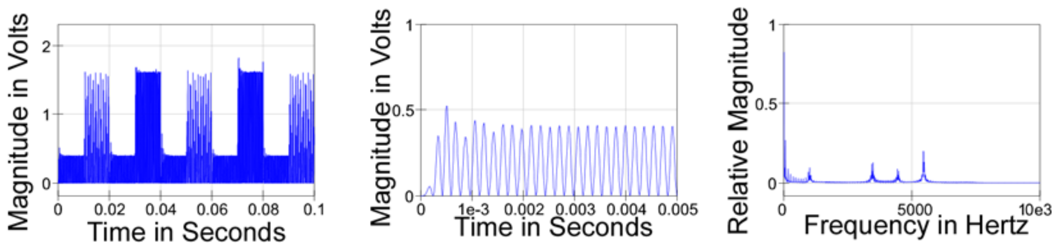

Figure 16.2 *Vout* Squared, a Detail, and the Spectrum

In figure 16.3 below, we see that we can utilize a narrow-bandwidth filter and retrieve a replica of the 4400 Hz tone.

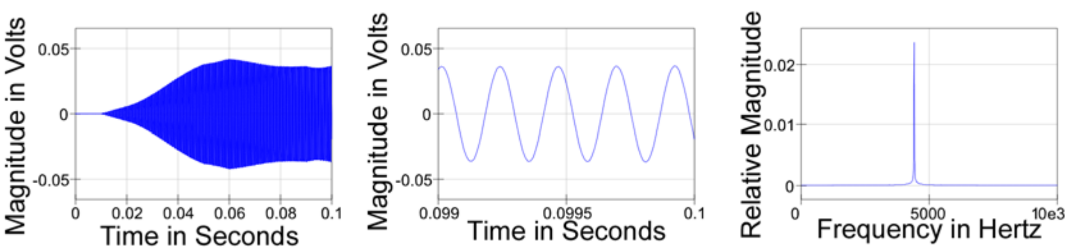

Figure 16.3 Band pass Filtered *Vout* Squared, a Detail, and the Spectrum

We have recovered a signal at 4400 Hz from the algebraically squared ***Vout*** signal that we discuss for timing purposes.

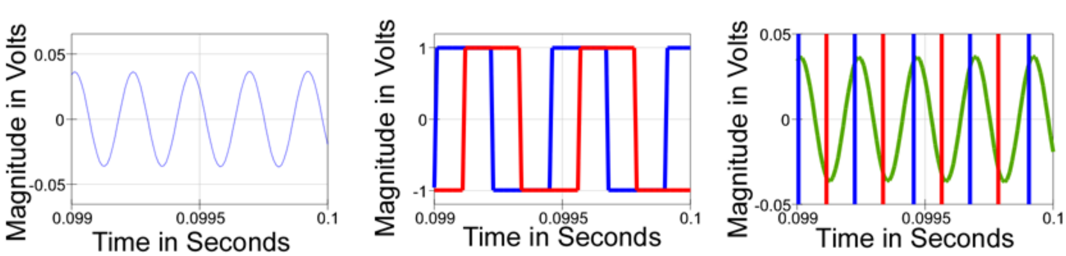

Figure 16.4 Band pass Filtered *Vout* Squared, *VRec_i* and ***VRec_q*, and the Compare**

 Copyright© 2010 Raymond L. Barrett, Jr.

In the previous figure 16.2, we saw that the ***Vout*** signal is always positive from its algebraic properties. The 4400 Hz minima occur whenever the originating 2200 Hz reference frequency passes through zero (twice per cycle, once rising and once falling). The band pass filtered 4400 Hz signal minima are representative of the same timing events. We see in figure 16.4 above that the edges of the ***VRec_i*** signal are nearly aligned with those minima, and the edges of the ***VRec_q*** signal are nearly aligned with the maxima. We are uncertain, however which signifies phase coherence, but we are assured that we are at the correct frequency.

The squaring and filtering approach is relatively primitive, but effectively makes the point that the requisite information is contained in the channel signal for frequency coherence. The more modern approach is to employ a Phase-Lock Loop (PLL) in an arrangement attributed to Costas for retrieval of the quadrature ***VRec_i*** and ***VRec_q*** signals from the Double-Sideband, Suppressed Carrier signal.

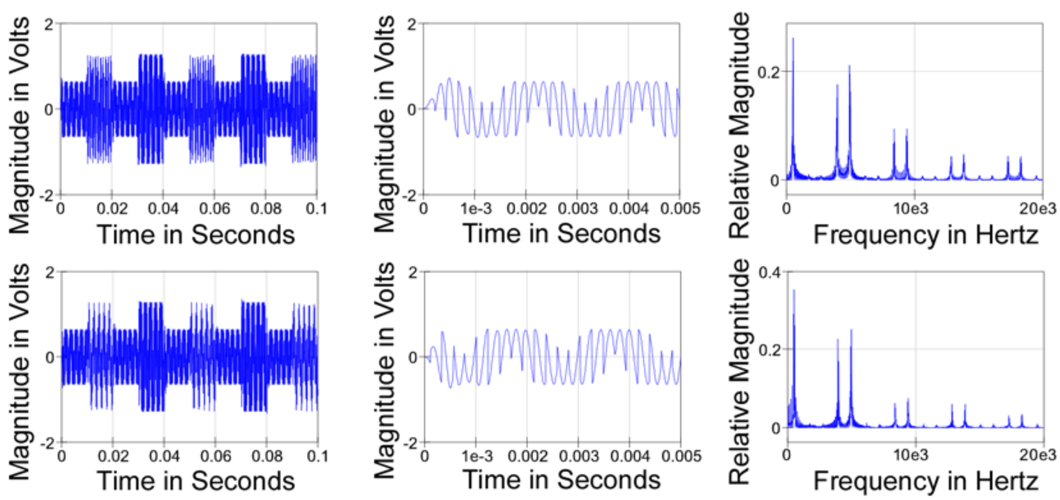

Figure 16.5 *VIFi* above *VIFq* below, Details, and Spectra

In figure 16.5 above, we see the result of modulating the channel signal by the ***VRec_i*** and ***VRec_q*** signals. We produce the expected 500 Hz difference signals as well as higher order harmonics.

Careful examination of the traces in figure 16.6 below show that the 500 Hz modulation in phase and amplitude are reproduced in the receiver *I* and *Q* signals and await signal processing to strip the amplitude and phase changes from each data stream.

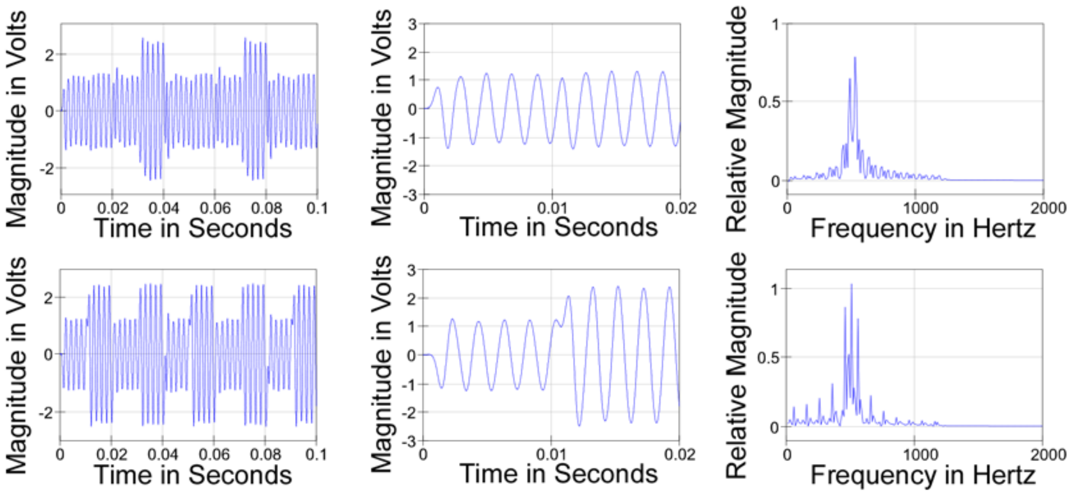

Figure 16.6 *V500R_i* above *V500R_q* below, Details, and Spectra

In figure 16.7 below, we show that variations of the phase of one square wave can make one channel respond to either modulation pattern and that phase coherence between the transmitter and receiver is necessary to reliably separate the *I* and *Q* channel information at the receiver.

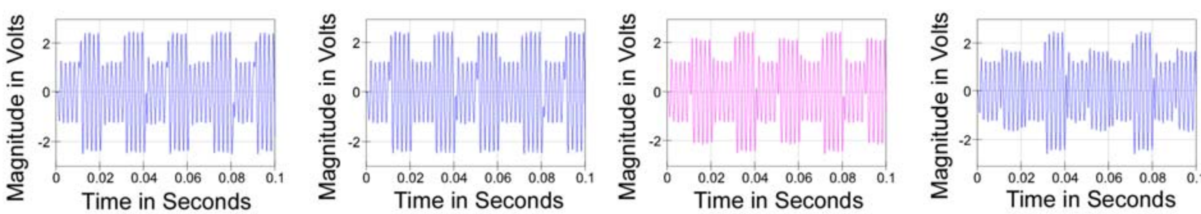

Figure 16.7 *V500R_q* Only with Four Differing Phase Values over a 90° Degree Range

17.0 Summary and Conclusions

This course introduced analog and digital communications concepts and some of the reasons for the migration from analog to digital technologies. Pertinent analog signal and system concepts were reviewed for comparison and contrast to corresponding digital concepts. Digital representation of analog signals was introduced in both the time and frequency domains so that analog transmission of digital signals could be compared. Versions of "Suppressed Carrier" modulation progressing from the original Weaver modulator architecture developed for "Single-Sideband, Suppressed Carrier" analog voice applications through variations to other applications. We added the phase modulation and amplitude

 Copyright© 2010 Raymond L. Barrett, Jr.

modulation to the Weaver architecture showing the development of quadrature techniques for using both upper and lower Weaver sidebands to produce independent "I" and "Q" communications channels. Only one bit of information is discussed for each of the phase modulation and amplitude modulation in a simple QAM example, but the groundwork is laid for extending the system. The concept of symbol rate and bit rates was introduced. The importance of frequency and phase synchronization of the receiving Weaver modulator was introduced and examples of issues discussed.

 Copyright© 2010 Raymond L. Barrett, Jr.